Improving parameter regionalization learning for spatialized differentiable hydrological models by assimilation of satellite-based soil moisture data

Mouad Ettalbi, Pierre-André Garambois, Ngo-Nghi-Truyen Huynh, Patrick Arnaud, Emmanuel Ferreira, Nicolas Baghdadi

Journal of Hydrology 660 (2025) 133300

Contents lists available at ScienceDirect

Journal of Hydrology

journal homepage: www.elsevier.com/locate/jhydrol

Research papers

Improving parameter regionalization learning for spatialized differentiable hydrological models by assimilation of satellite-based soil moisture data

Mouad Ettalbi [a,b,c,*], Pierre-André Garambois [a,*], Ngo-Nghi-Truyen Huynh [a], Patrick Arnaud [a], Emmanuel Ferreira [c], Nicolas Baghdadi [b]

[a] INRAE, UMR RECOVER, Aix-Marseille Université, Aix-en-Provence, 13182, France
[b] INRAE, UMR TETIS, Université de Montpellier, Montpellier, 34090, France
[c] AIWAY, Aix-en-Provence, 13851, France

ARTICLE INFO

This manuscript was handled by Marco Borga, Editor-in-Chief, with the assistance of Luca Brocca, Associate Editor.

Keywords:
Spatialized differentiable hydrological model
Learnable regionalization
Adjoint model
Floods
Variational data assimilation
Satellite moisture
SMAP L4 data

ABSTRACT

Accurate and high-resolution hydrological models are crucially needed, especially for important socioeconomic issues related to floods and droughts, but are faced with data and model uncertainties which can be reduced by maximizing information integration from multisource data. This work focuses on improving the integration of satellite and in situ land surface data into spatially distributed hydrological models. The Hybrid Data Assimilation and Parameter Regionalization (HDA-PR) approach incorporating learnable regionalization mappings, based on neural networks into the differentiable spatially distributed hydrological model SMASH, is modified to account for satellite-based moisture maps in addition to discharge at gauging stations and basin physical descriptors maps. Regional optimizations of a spatially distributed conceptual model are performed on a flash-flood-prone area located in the South of France, and their accuracy and robustness are evaluated in terms of simulated discharge and moisture against observations. In general, the integration of satellite-derived soil moisture data alongside traditional observed streamflow measurements during calibration procedures has demonstrated notable improvements in hydrological performance, both in terms of simulated discharge and moisture. This is achieved thanks to an improved learning of regionalization of model conceptual parameters with HDA-PR integrating satellite-based moisture through the RMSE metric adapted to a spatially distributed model with variational data assimilation. This study provides a solid foundation for advanced data assimilation of multi-source data into learnable spatially distributed differentiable geophysical models.

1. Introduction

Water is the lifeblood of our Earth, supporting ecosystems and human societies alike (Kherazi et al., 2024). With the intensification of climate change, the need for precise and reliable forecasts of hydrological states and flows has never been more critical (Fowler et al., 2021; Ficklin et al., 2022; Guerreiro et al., 2018). Accurate hydrological predictions are essential for the effective management of water resources, societal resilience, and the mitigation of natural disasters (Lavers et al., 2020; Bou-Fakhreddine et al., 2018; Kim et al., 2024). Flash floods, characterized by their rapid onset and devastating impact, highlight the need for advanced modeling techniques that integrate diverse data sources to improve forecast precision and reliability (Marchi et al., 2010).

The advent of increasing multisatellite data presents unprecedented opportunities to improve our understanding and prediction of hydrological processes (McCabe et al., 2017). Satellite observations provide comprehensive and high-resolution data on various hydrological variables (Brocca et al., 2023), such as soil moisture (Peng et al., 2021), precipitation (Schneider et al., 2013), and land surface characteristics (Köhler and Kuenzer, 2020). However, the volume and complexity of these data necessitate the development of powerful data-model fusion methods to effectively assimilate this information into hydrological models. Advanced data assimilation techniques, which integrate satellite with model predictions, are essential to reduce uncertainties and improve the accuracy of forecasts (Reichle, 2008). However, integrating models with observational data is fraught with complexities and challenges, primarily due to various sources of uncertainty. These uncertainties arise from errors in both the data and the models themselves (Renard et al., 2010). Data errors can stem from measurement inaccuracies, spatial and temporal inconsistencies, and sensor limitations (Mcmillan et al., 2022). Model errors, on the other hand, often result from structural inadequacies and the inherent empirical nature

* Corresponding authors.
E-mail addresses: mouad.ettalbi@aiway.fr (M. Ettalbi), pierre-andre.garambois@inrae.fr (P.-A. Garambois).

https://doi.org/10.1016/j.jhydrol.2025.133300
Received 17 October 2024; Received in revised form 12 March 2025; Accepted 10 April 2025
Available online 25 April 2025

Table 1
Summary of the literature review on studies assimilating satellite-derived soil moisture data for parameter estimation in hydrological models for flood forecasting.

Reference	Model	Data used	Assimilation algorithm	Calibration metric	Model resolution
Tramblay et al. (2010)	SCS–CN	SIM-ISBA	Nelder–Mead	Initial conditions	30min-lumped
Wanders et al. (2014)	LISFLOOD	AMSR-E, SMOS, and ASCAT	EnKF	Covariance	Daily-12.5 km
Cenci et al. (2017)	Continuum	Sentinel 1 and ASCAT	Parallel search	Nudging	Hourly-100 m
Massari et al. (2018)	MISDc	ASCAT	EnKF	Covariance	Daily-lumped
Zhou et al. (2020)	VIC	SMAP	Newton–Raphson	Bias correction	Daily-5 km
Yi et al. (2021)	WRF-TOPX	SMAP	4D-Var	Covariance	Hourly-1 km
Jadidoleslam et al. (2021)	HLM	SMOS and SMAP	EnKF	Covariance	Hourly-semi-distributed
Meyer Oliveira et al. (2021)	MGB	SMOS	MOCOM-UA	Averaged KGE	Daily-lumped
Le et al. (2022)	SWAT	SMAP	EnKF	Covariance	Daily-1 km
Chao et al. (2022)	WRF-Hydro	SMAP, SMOS, AMSR2, and Fengyun	EnKF	Bias correction	Hourly-1 km
Alfieri et al. (2022)	Continuum	Sentinel-1	Parallel search	Nudging	Hourly-1 km
Ding et al. (2022)	MISDc	CLDAS-BPNN	EnKF	Covariance	Daily-lumped
Wakigari and Leconte (2023)	HYDROTEL	SMAP	DDS	Direct insertion	Daily-semi-distributed
Li et al. (2023)	GBHM	SMAP	ESTKF	Bias correction	Daily-600 m
Bechtold et al. (2023)	Noah-MP-Hymap	Sentinel-1 backscatter	EnKF	Forward operator	Daily-1 km

of many hydrological models (Messina et al., 2008), which are based on approximations and assumptions due to an incomplete understanding of the underlying physical laws (Beven, 1987). Moreover, due to the sparsity of constraining discharge observations with respect to the spatially distributed parameters to estimate, satellite moisture, which is a partial but spatialized observation of catchment hydrological response is interesting in view of reducing the uncertainty of the modeling. The data assimilation process in hydrology is further complicated by the wide range of possible solutions and the heterogeneous nature of hydrological systems (Houser et al., 2012). Empirical models frequently exhibit significant variability in their predictions, reflecting the vast parameter space and the diverse environmental conditions they attempt to simulate (Koo et al., 2020). This variability underscores the need for robust assimilation techniques that can handle these uncertainties and effectively integrate disparate data sources to improve model accuracy and reliability. Data assimilation is a constantly evolving field that works to bridge the gap between, for example, the complexities of real-world hydrology and the predictive power of computational models (Castelli, 2023). It is an area that draws on a wide range of methods and data sources with the aim for better understanding and forecasting the behavior of water systems in all their complexity (see Table 1).

Soil moisture data is a critical component of hydrological modeling, influencing numerous hydrological and climatic processes (Reichle, 2008). This data is obtained through a variety of sensors and platforms, including ground-based captors and advanced satellite missions such as Sentinel (Baghdadi et al., 2001; Zribi and Dechambre, 2003; El Hajj et al., 2017), SMOS (Soil Moisture and Ocean Salinity) (Kerr et al., 2001), and SMAP (Soil Moisture Active Passive) (Entekhabi et al., 2010). These satellites deliver high-resolution, global measurements, while ground-based sensors provide localized, high-frequency data essential for the validation and calibration of satellite observations. In parallel, land surface models (LSMs) such as VIC (Variable Infiltration Capacity) (Liang et al., 1994), Noah-MP (Multi-Parameterization) (Niu et al., 2011), and CLM (Community Land Model) (Lawrence et al., 2019) synthesize hydrological and meteorological data to simulate soil moisture dynamics. By integrating observational data with advanced algorithms, these models estimate soil moisture and other land surface variables more accurately, thereby improving hydrological forecasts.

The assimilation of satellite-derived soil moisture data into hydrological models has been shown to significantly improve the calibration of model parameters, reducing uncertainties and improving the simulation of hydrological processes (Wanders et al., 2014; Jadidoleslam et al., 2021). This approach is particularly beneficial for improving the accuracy of runoff predictions and flood forecasting (Massari et al., 2018; Chao et al., 2022). Furthermore, the integration of remote sensing data has proven valuable in addressing challenges in ungauged or sparsely gauged regions, where traditional ground-based measurements are limited (Dembélé et al., 2020). Recent advances in remote sensing technologies, such as the use of Sentinel-1, SMAP, and AMSR-E, have further enhanced the ability to monitor soil moisture dynamics with high resolution and precision (Zhou et al., 2020; Li et al., 2023). These advances have been instrumental in the refinement of hydrological models, leading to more reliable predictions of water availability and flood risks (Le et al., 2022; Bechtold et al., 2023). Recent developments in hydrological modeling have emphasized the integration of satellite-derived soil moisture data through various data assimilation techniques. One widely used approach is the Ensemble Kalman Filter (EnKF), which has shown improvements in the accuracy of flood forecasting by assimilating data from satellites such as AMSR-E, SMOS, and ASCAT into models like LISFLOOD and MISDc (Wanders et al., 2014; Massari et al., 2018). Parallel search algorithms and nudging techniques have also been applied in studies using Sentinel-1 and ASCAT data, especially with the Continuum model, to refine parameter estimations and enhance flood prediction capabilities (Cenci et al., 2017; Alfieri et al., 2022). Moreover, models integrating multiple satellite data sources, such as SMAP, SMOS, AMSR2, and Fengyun in the WRF-Hydro model, utilize EnKF for bias correction and achieve robust flood forecasting (Chao et al., 2022). Furthermore, variational data assimilation (VDA) methods like 4D-Var have been implemented with SMAP data in models such as WRF-TOPX, contributing to better overall model performance (Yi et al., 2021). While the integration of soil moisture data in data assimilation frameworks has been established in hydrological modeling, existing approaches have several limitations, particularly in addressing equifinality, robustness, and parameter regionalization in complex, spatially distributed hydrological systems. From the extensive literature review, three key patterns emerge in current methodologies.

Most studies utilize Ensemble Kalman Filter (EnKF) approaches, as demonstrated in the work of Wanders et al. (2014), Massari et al. (2018), and Le et al. (2022). The LISFLOOD model with AMSR-E, SMOS, and ASCAT data operates at daily 12.5 km resolution, while the SWAT model integrating SMAP data functions at daily 1 km resolution. These ensemble methods, while effective for uncertainty quantification, often struggle with computational efficiency at higher resolutions and in inferring spatially distributed parameters.

Current models predominantly operate at relatively coarse spatiotemporal scales. Many use daily timesteps, such as VIC with 5 km resolution (Zhou et al., 2020), or employ semi-distributed approaches like HYDROTEL with SMAP data (Wakigari and Leconte, 2023). Some rely on lumped models, as seen in MISDc with ASCAT (Massari et al., 2018). Few models attempt to integrate soil moisture data at both high spatial and temporal resolutions. The Continuum model (Alfieri et al., 2022) achieves hourly-1 km resolution but relies on simpler nudging techniques for moisture data assimilation to correct model states. Additionally, a few lumped hydrological parameters are precalibrated separately using discharge data. However, the WRF-Hydro's

computational demands and complexity pose challenges for operational high-resolution applications.

Parameter regionalization integration remains limited in current approaches, which typically handle parameter estimation and state correction by data assimilation as separate processes. Models like WRF-TOPX (Yi et al., 2021) employ 4D-Var of satellite rainfall, but without learnable regionalization, while the GBHM model (Li et al., 2023) uses ESTKF at 600 m resolution for satellite moisture assimilation but lacks sophisticated parameter transfer schemes.

The integration of satellite-based soil moisture and multi-gauge discharge within a hybrid variational data assimilation (VDA) framework remains largely unexplored, particularly when combined with learnable parameter regionalization at high spatiotemporal resolutions. This gap is especially significant considering the need for robust parameter estimation in complex spatially-distributed systems and the challenges of flash flood prediction requiring fine spatiotemporal resolution. The potential of machine learning-based regionalization to improve parameter learning from multi-source data and the computational efficiency advantages of variational approaches over ensemble methods for parameter optimization at high resolutions further underscore the importance of addressing these limitations.

While some studies have attempted to bridge these gaps individually — such as WRF-Hydro's integration of multiple satellite sources at hourly-1 km resolution (Chao et al., 2022) or the Continuum model's use of Sentinel-1 data (Alfieri et al., 2022) - none have comprehensively addressed the combination of high-resolution spatiotemporal modeling, hybrid variational data assimilation, learnable parameter regionalization from physical descriptors, and multiple constraint integration through discharge and soil moisture data. This comprehensive gap in the literature underscores the novelty of our proposed approach, which aims to advance the field by addressing these limitations through a unified framework.

This development not only highlights the current state of the field but also clearly positions the novel contributions of the proposed methodology within the broader context of hydrological modeling and data assimilation. The integration of these advanced techniques promises to overcome existing limitations and provide more robust and accurate hydrological predictions at the high resolutions necessary for practical applications such as flash flood forecasting.

In this context, the Hybrid Data Assimilation-Parameter Regionalization (HDA-PR) approach (Huynh et al., 2024) offers a promising advancement. By combining the strengths of variational data assimilation (VDA) with a learnable descriptors-to-parameters mapping, HDA-PR enables more precise spatialization of parameters across large domains. This hybrid method is designed to tackle the key challenges of model robustness and equifinality, which have traditionally limited the effectiveness of hydrological models, especially in ungauged or sparsely gauged regions. Integrating SM data into this framework is crucial because it directly constrains the hydrological response inside basins, addressing spatial inconsistencies that remain unresolved by discharge observations alone.

This article presents a novel approach in hydrological modeling, centered on the variational data assimilation (VDA) of discharge (Q) and spatialized soil moisture (SM) into a fully distributed differentiable hydrological model containing a learnable descriptors-to-parameters regionalization mapping, at high spatiotemporal resolutions. It demonstrates how this technique performs under different calibration strategies and provides a systematic evaluation of its strengths and limitations. We employ various metrics to account for soil moisture, addressing the complexities of accurately representing this critical hydrological variable. A key aspect of the research is the investigation of multi-objective calibration concerning both discharge (Q) and soil moisture (SM). This study analyzes the regionalization and the spatiotemporal validation capacity of the model, highlighting the improvements achieved in simulating these quantities. By integrating VDA techniques and examining their impact on model performance, this work provides valuable insight into improving the reliability and accuracy of hydrological forecasts, especially in the context of regionalized hydrological modeling.

2. Study area

Positioned within the varied topographies of southern France (Fig. 1), our study area holds considerable hydrological importance due to its vulnerability to extreme events, including floods and droughts. Characterized by diverse climatic, physiographic, and land use attributes, the study area epitomizes a heterogeneous hydrological landscape. The region's susceptibility to flash-flood events underscores the imperative for advanced modeling tools capable of precise and reliable local forecasts, particularly amidst the ongoing challenges posed by global climate change.

A total of 128 catchments are included in our analysis, providing a comprehensive spatial representation across the study area. These catchments exhibit significant variability in size, with areas ranging from a minimum of 28 km^2 to a maximum of 1958 km^2 (Table 2), contributing to the complexity of hydrological processes within the region. Topographically, the study area showcases a spectrum of features, including steep slopes in mountainous regions, gentle hills, and flat plains, influencing precipitation patterns, runoff generation, and streamflow dynamics.

Climatic conditions within the catchments are diverse, with mean annual precipitation ranging from 510.94 mm/year to 1552.75 mm/year and mean annual potential evapotranspiration ranging from 490.32 to 883.08 mm/year. Additionally, the catchments exhibit a range of aridity index values, spanning from 0.60 to 2.71, reflecting the overall water balance within the catchments.

In summary, the study area presents a complex hydrological landscape characterized by diverse catchment attributes, including size, topography, climatic conditions, and land use/land cover patterns. Given the wide range of catchments with highly contrasting physical properties and their nonlinear, complex hydrological responses, this region presents a challenging case for testing soil moisture assimilation with our algorithm.

3. Data sets

This section provides a comprehensive overview of the datasets utilized to calibrate and validate our models, including an examination of their sources, characteristics, and spatio-temporal samplings. The analysis period for all dynamic forcings spans from August 1, 2015, to August 1, 2023, partitioned into calibration (from August 1, 2015, to August 1, 2019) and validation periods (from August 1, 2019, to August 1, 2023). The discharge gauges are further divided into two groups, gauges used for calibration and gauges used for spatial validation (to evaluate the model's regionalization function).

Discharge time series at gauged sites are obtained from the national banque hydro (http://www.hydro.eaufrance.fr/) with an hourly temporal resolution from August 1, 2015, to August 1, 2023. Hydroportail is an online platform provided by the French Ministry of Ecological Transition and Solidarity. It serves as a centralized hub for accessing hydrological and hydraulic information related to water resources in France.

Observed rainfall grids are derived from the ANTILOPE J+1 radar-gauge rainfall reanalysis dataset provided by Météo-France. This dataset combines radar observations with in-situ gauge measurements to estimate high-resolution rainfall. The reanalysis process integrates hourly data from radar and gauge sources to generate hourly gridded rainfall fields, providing spatially continuous precipitation coverage over the study area. The grid cells used have a spatial resolution of 1×1 km^2, allowing for a detailed representation of precipitation patterns at a local scale.

The interannual temperature data used for calculating potential evapotranspiration (PET) originates from the SAFRAN reanalysis dataset developed by Météo-France (Quintana-Seguí et al., 2008). This dataset integrates observational data from ground-based weather stations, satellite observations, and numerical weather prediction models. Downscaled to a 1×1 km^2 spatial grid, the SAFRAN reanalysis provides

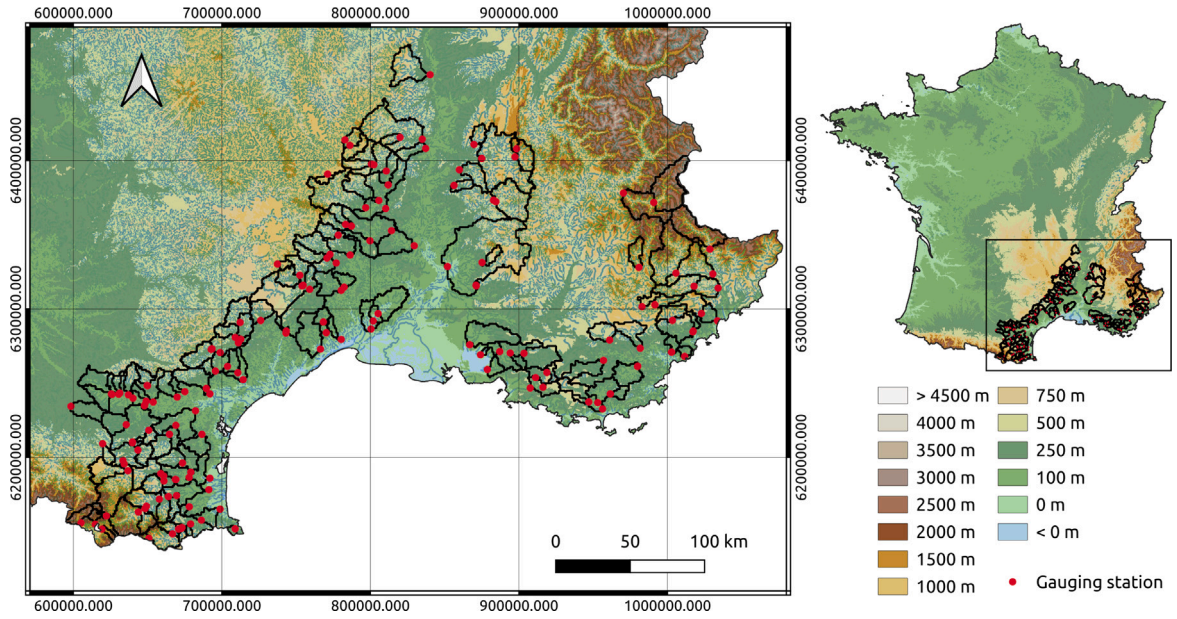

Fig. 1. Topographic overview of the study region delineating the locations of the 128 catchments examined in this study, along with the positions of their respective discharge gauging stations.

Table 2
Summary of hydrologic, climatic and physiographic catchment attributes.

Catchment characteristic	Unit	Min.	Max.	Median	STD
Area	km^2	28	1958	239	415.25
Mean annual precipitation (P)	mm/year	510.94	1552.75	821.82	248.74
Mean annual potential evapotranspiration (PET)	mm/year	490.32	883.08	741.46	87.82
Catchment aridity index (P/PET)	–	0.60	2.61	1.17	0.45
Mean soil moisture saturation	%	25.87	46.63	37.29	5.28
Mean hourly discharge	m^3/s	0.06	49.16	2.45	7.22
Mean catchment slope	°	0.01	5.35	2.01	1.32
Drainage density	–	9.82	28.94	17.76	3.50
Percentage of catchment in karst zone	%	0	100	36.61	34.26
Forest cover rate	%	7.45	94.07	55.30	21.65
Urban cover rate	%	0	50.72	1.85	7.45
Potential available water reserve	mm	48.00	327.47	200.15	51.62
High storage capacity rate	%	0	82.46	0.02	20.30

detailed temperature information across the study area . Utilizing this enhanced temperature dataset, hourly PET at 1×1 km^2 is calculated employing the Oudin formula (Oudin et al., 2005).

A set of 7 temporally static physical descriptors available over the whole French territory is used following Odry (2017), Jay-Allemand et al. (2024), Huynh et al. (2024). These descriptors are Slope, Drainage density, Percentage of the basin area in karst zone, Forest and urban cover rate, Potential available water reserve and High storage capacity basin rate.

The soil moisture data utilized in this study is sourced from the SMAP level 4 dataset, which provides soil moisture data up to the bedrock, expressed as a percentage and obtained by assimilation of SMAP data into a physically-based numerical model of the land surface water, energy, and carbon cycles (Reichle et al., 2019). This dataset offers valuable insights into soil moisture dynamics, with a spatial resolution of approximately 9 km and a temporal resolution of 3 h. This data was downscaled to a 1×1 km^2 spatial grid using the nearest neighbor to match it with the hydrological model's spatial resolution.

4. Gridded hydrological model and hybrid data assimilation algorithm

Hybrid Data Assimilation and Parameter Regionalization (HDA-PR) algorithm (Huynh et al., 2024) is based on (i) a forward model consisting of a differentiable spatially distributed continuous hydrological model embedding an NN-regionalization pipeline for mapping physiographic descriptors onto hydrological model parameters, (ii) and an adjoint-based variational data assimilation algorithm as illustrated in 2.

HDA-PR uses a forward model $\mathcal{M}$ that combines:

- $\mathcal{M}_{rr}$ a spatially distributed and differentiable GR4 conceptual structure adapted from Jay-Allemand et al. (2020) called SMASH for Spatially-distributed Modeling and Assimilation for Hydrology, this model projects rainfall fields $\boldsymbol{P}$ and potential evapotranspiration fields $\boldsymbol{E}$ onto discharge and states fields, respectively $\boldsymbol{Q}$ and $\boldsymbol{h}$ factoring in drainage plans $\mathcal{D}_\Omega$ and spatially varying parameters $\boldsymbol{\theta}$. The model is defined for all spatial locations $x \in \Omega$ and times $t' \in [0, t]$, where Ω represents the 2D spatial domain and $t > 0$ is the physical time. In a discretized representation, x corresponds to a pixel in the computational grid, such that, $\forall (x, t') \in \Omega \times [0, t]$:

$$\boldsymbol{Y}(x, t; \boldsymbol{\theta}) = (\boldsymbol{h}, \boldsymbol{Q})(x, t) = \mathcal{M}_{rr}\left[(\mathcal{D}_\Omega, \boldsymbol{\theta})(x); (\boldsymbol{P}, \boldsymbol{E})(x, t'), \boldsymbol{h}(x, 0), t\right] \tag{1}$$

$$\boldsymbol{\theta}(x) = \left(C_p(x), C_t(x), k_{exc}(x), l_r(x)\right)^T \tag{2}$$

$$\boldsymbol{h} = \left(h_p, h_t\right)(x, t) \tag{3}$$

where the four spatially varying parameter fields that the model aims to estimate regionally are the maximum capacity of the

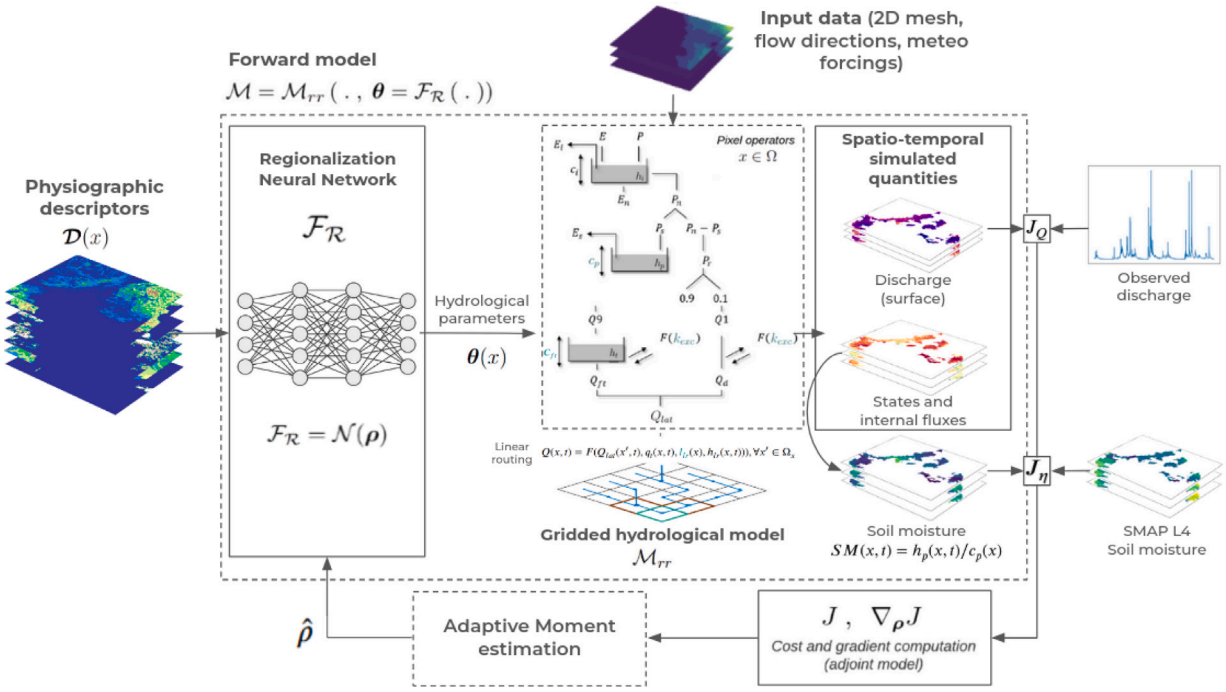

Fig. 2. Flowchart of the forward-inverse algorithm used in HDA-PR with satellite moisture based data assimilation. The forward hydrological model is a gridded model (spatio-temporal regular grid at 1 km^2 and 1 h) using GR operators.

production reservoir (C_p in [mm]), the maximum capacity of the transfer reservoir (C_t in [mm]), the parameter of the non-conservative water exchange flux (k_{exc} in [mm/dt]), and the linear routing parameter (l_r in [min]). Where h_p and h_t (in [mm]) are respectively the states of the production and transfer reservoirs.

- $\mathcal{F}_R$ the regionalization operator that maps the physiographic descriptors $\boldsymbol{D}$ to conceptual hydrological parameters $\boldsymbol{\theta}$, using an artificial neural network (ANN) $\mathcal{N}$ learning the mapping through a multilayer perceptron architecture, such that, $\forall x \in \Omega$:

$$\boldsymbol{\theta}(x) = \mathcal{F}_R(\boldsymbol{D}(x), \boldsymbol{\rho}) \tag{4}$$

$$\boldsymbol{\theta}(x, \boldsymbol{D}, \boldsymbol{\rho}) = \mathcal{N}(\boldsymbol{D}(x), \boldsymbol{W}, \boldsymbol{b}) \tag{5}$$

with $\boldsymbol{D}$ the N_D-dimensional vector of physical descriptor maps covering Ω, and $\boldsymbol{\rho}$ the vector of regionalization parameters composed of $\boldsymbol{W}$ and $\boldsymbol{b}$ which are respectively weights and biases of the neural network.

In this study, we explore a novel multi-objective cost function for the HDA-PR approach, incorporating SMAP satellite soil moisture observations alongside traditional discharge data. We compare this multi-objective approach with the conventional single-objective cost function, which relies solely on discharge information. The classical HDA-PR single-objective cost function for multiple gauging stations is formulated as :

$$J_Q = \frac{1}{N_g} \sum_{g=1}^{N_g} (1 - NSE(Q_g^*(t), Q_g(t))) \tag{6}$$

with N_g the number of gauging stations, $Q_g^*(t)$ the observed discharge time series at gauging station g, $Q_g(t)$ the estimated discharge time series at gauging station g by the forward model $\mathcal{M}$, and NSE is the Nash–Sutcliffe efficiency coefficient between observed and estimated data.

In the new multi-objective cost function, the measure of the difference between the modeled and observed variables is done using the following cost function:

$$J = J_Q^2 + J_\eta^2 \tag{7}$$

with J_Q the classical discharge observation term from (6) and J_η a soil moisture saturation observation term related to satellite snapshots. Consequently, J_Q should ensure a reliable prediction of streamflow signatures, particularly high flows, due to the NSE's tendency to emphasize larger errors more than smaller ones (Legates and McCabe, 1999; Krause et al., 2005; Gupta et al., 2009). J_η serves to improve the spatial patterns of the modeled soil moisture by constraining the optimization of the spatially distributed model parameters, thus reducing parameter equifinality and making the calibration process more robust.

In what follows, we use SMAP L4 soil moisture (SM) data, which have been obtained by merging SMAP surface moisture measurements into a large-scale LSM model by assimilation with a spatially distributed ensemble Kalman filter (Reichle et al., 2017, 2019). We choose to use these data because (i) they are available at the global scale at 9 km and 3 h spatial and temporal resolution, (ii) they consist of satellite-based validated soil moisture estimates obtained with state-of-the-art LSM model with DA framework. As our conceptual model contains a soil moisture accounting GR production reservoir, we assume that this satellite-based soil moisture data $SM^*(x,t)$, a moisture rate between 0 and 1 and projected onto our numerical grid, is directly comparable to the normalized production state of our production reservoir:

$$SM(x,t) = h_p(x,t)/C_p(x) \tag{8}$$

In other words, we assume the observation operator for this moisture product to be the identity.

The choice of a calibration metric for soil moisture data is difficult, usually the metric of choice when it comes to lumped models is some variation of the NSE or KGE on spatially averaged remote sensing data (Liu et al., 2022; Meyer Oliveira et al., 2021; Wang et al., 2023), while this approach shows general increase in the discharge's estimation precision, these metrics do not fully capture the spatial heterogeneity that remotely sensed data can offer. In the case of distributed hydrological modeling, a lot of interest has been shown towards bias-insensitive spatial pattern metrics (Demirel et al., 2018; Dembélé et al., 2020; Zink et al., 2018), overall the simulated spatial patterns of the calibrated parameters show a similarity with the satellite observations, however, this comes with a trade-off between discharge

precision and spatial patterns, especially for soil moisture calibration. For these reasons, we chose to evaluate two soil moisture calibration metrics. The first is the root mean squared error between observed and estimated soil moisture, J_η^{RMSE}, giving us a global metric of pixel-by-pixel discrepancy between simulated and observed moisture through time. It can be seen as a lump-like metric without weighting in space and time. The second is the spatial bias insensitive metric from Dembélé et al. (2020) to take advantage of the spatial information in the SMAP L4 data. This metric is formulated as follows:

$$J_\eta^{SP} = 1 - \frac{1}{T}\sum_{\substack{t=1 \\ \forall i,j\in\Omega}}^{T}(1 - E_{SP}(SM^{*t}(i,j), SM^{t}(i,j)))^2 \tag{9}$$

The degree of reproduction of spatial patterns is quantified with the following pattern matching metric, denoted E_{SP}, using observed and estimated soil moisture (SM and SM^*). The pattern matching metric E_{SP} is defined as follows:

$$E_{SP} = 1 - \sqrt{(r_s - 1)^2 + (\gamma - 1)^2 + (\alpha - 1)^2}, \quad with \tag{10}$$

$$r_s = \rho\left(SM^*, SM\right) \equiv \frac{\langle SM^*, SM\rangle}{\|SM^*\|\,\|SM\|} \tag{11}$$

$$\gamma = \frac{\frac{\sigma_{est}}{\mu_{est}}}{\frac{\sigma_{obs}}{\mu_{obs}}}, \tag{12}$$

$$\alpha = 1 - E_{MSE}(Z_{SM^*}, Z_{SM}), \tag{13}$$

where r_s is the Spearman rank-order correlation coefficient between estimated soil moisture SM^* and observed soil moisture SM, γ is the variability ratio that assesses the similarity in the dispersion of the probability distribution of SM^* and SM, with μ and σ representing the mean and the standard deviation, and α the spatial matching term.

The variational data assimilation approach (VDA) aims at combining the forward model $\mathcal{M}$, composed of the descriptors-to-parameters mapping $\mathcal{F}_R$ and of the spatially distributed hydrological model $\mathcal{M}_{rr}$, with the multi-site discharge time series and soil moisture maps in the sense of the cost function defined above. This multi objective cost function J (Eq. (7)) depends on the sought parameter $\boldsymbol{\rho}$ of the regionalization neural network $\mathcal{F}_R$ embedded into the hydrological model through model response $\boldsymbol{Y}(\boldsymbol{\rho}) = (\boldsymbol{h}, Q)(\boldsymbol{\rho})$ in terms of discharge Q and soil moisture SM here accounted in the cost function (cf. Eq. (6) to (9)). The VDA optimization problem reads:

$$\hat{\boldsymbol{\rho}} = \arg\min_{\boldsymbol{\rho}} J\left(\boldsymbol{Y}\left(\boldsymbol{\rho}\right)\right) \tag{14}$$

with $\boldsymbol{\rho}$ the parameters of the regionalization neural network operator when used, otherwise $\boldsymbol{\rho} \equiv \boldsymbol{\theta}(x)$ and the spatially distributed conceptual hydrological parameters are inferred directly. This problem is solved with adaptive moment ADAM (resp. LBFGS-B) algorithm in case "HDA-PR" of regionalization mapping $\boldsymbol{\rho} = (\boldsymbol{W}, \boldsymbol{b})$ (resp. case "CDC" classical distributed calibration $\boldsymbol{\rho} \equiv \boldsymbol{\theta}(x)$). Both algorithms take advantage of cost gradients with respect to the sought parameter, $\nabla_{\boldsymbol{\rho}} J$ given by the resolution of the numerical adjoint model $D_{\boldsymbol{\rho}}\mathcal{M}$ obtained by automatic differentiation of the source code (cf. Huynh et al. (2024) and references therein). The strength of HDA-PR lies in the use of a regionalization neural network to infer unknown descriptors-to-parameters mapping while remaining interpretable in conceptual parameter space. The proposed modification of HDA-PR makes it amenable to assimilate satellite-based soil moisture product.

5. Experimental design

In this section, we detail our experimental setup devised to evaluate the benefits of integrating soil moisture data into the calibration process alongside discharge data. We examine the impact of this enhanced calibration approach on two different configurations, CDC (i.e SMASH with Classical Distributed Calibration) and HDA-PR (i.e. SMASH with descriptors-to-parameters learnable regionalization mapping). For each model, we perform comparative analyses by evaluating the calibration with soil moisture using the two metrics presented in the previous section, the root mean square error (RMSE) and the spatial bias insensitive metric (SP).

The Classical Distributed Calibration approach uses a gradient-based optimization algorithm (L-BFGS-B) to minimize the objective function J, which combines discharge error (J_Q) and soil moisture error (J_η). Regularization is omitted to focus on raw data fidelity. Parameter values are defined within physically plausible bounds derived from prior studies and expert knowledge:

- C_p **(maximum capacity of the production reservoir)**: The initial values are set to 200 mm, with calibration bounds of $C_p \in [1e-6, 1e3]$ mm.
- C_t **(maximum capacity of the transfer reservoir)**: The initial values are set to 500 mm, with calibration bounds of $C_t \in [1e-6, 1e3]$ mm.
- k_{exc} **(non-conservative water exchange flux)**: The initial values are set to 0, with calibration bounds of $k_{exc} \in [-50, 50]$ mm/dt.
- l_r **(linear routing parameter)**: The initial values are set to 5 min, with calibration bounds of $l_r \in [1e-6, 1e3]$ min.

These bounds are carefully chosen to ensure parameter realism, reflecting the physical constraints of hydrological processes. At the same time, they allow flexibility for catchment-specific adjustments, enabling the model to adapt to varying environmental conditions across different regions.

For the HDA-PR method, no background term is used since the regionalization mapping incorporated into the forward model provides a strong spatial constrain (cf. Huynh et al. (2024)). Although this study yields promising results, the estimation of observation error covariance matrices—useful for weighting observations in the cost function—remains challenging and is left for future research. We use the ADAM optimizer to optimize the neural network parameters. The weights of the network are initialized with a normal distribution with mean 0 and standard deviation of 0.01, while the biases are initialized to zero for each layer. This initialization scheme ensures that the network begins training with small, random weights that allow for effective learning.

In total, we compare 6 models: three models based on the traditional calibration method with distributed mapping (i.e., Jay-Allemand et al. (2020) without a regularization term) and three models based on the HDA-PR approach, as follows:

- **CDC without SM**: spatially distributed calibration of SMASH model parameters $\theta(x)$ solely with discharge data ($J \equiv J_Q$).
- **CDC with SM SP**: spatially distributed calibration of SMASH model parameters $\theta(x)$ using discharge data and spatial bias insensitive soil moisture calibration ($J \equiv J_Q + J_\eta^{SP}$).
- **CDC with SM RMSE**: spatially distributed calibration of SMASH model parameters $\theta(x)$ using discharge data and root mean squared error soil moisture calibration ($J \equiv J_Q + J_\eta^{RMSE}$).
- **HDA-PR without SM**: calibration of parameters $\boldsymbol{\rho}$ of the regionalization neural network $\mathcal{N}$ embedded into SMASH for physical-descriptors-to-parameters mapping, calibrated solely with discharge data.
- **HDA-PR with SM SP**: calibration of parameters $\boldsymbol{\rho}$ of the regionalization neural network $\mathcal{N}$ embedded into SMASH for physical-descriptors-to-parameters mapping, calibrated discharge data and spatial bias insensitive soil moisture calibration.
- **HDA-PR with SM RMSE**: calibration of parameters $\boldsymbol{\rho}$ of the regionalization neural network $\mathcal{N}$ embedded into SMASH for physical-descriptors-to-parameters mapping, calibrated discharge data and root mean squared error soil moisture calibration.

Each of these 6 models is calibrated using half of the catchments presented in Section 2 while the other half is used for spatial validation (ability of the model to estimate discharge for new catchments), the calibration period spans from 08-01-2015 to 08-01-2019 and the validation period spans from 08-01-2019 to 08-01-2023, the same catchments and periods are used for each model to have a fair assessment of the models. Using this setup, we can validate each model's temporal and spatial extrapolation capabilities.

Detailed analysis are conducted to evaluate the influence of satellite moisture data calibration on the performance of the hydrological models. Our analysis places particular emphasis on assessing both discharge precision in terms of discharge modeling at the selected gauges in the French Mediterranean region and coherence between observed and simulated moisture. To evaluate discharge precision, we employ the Nash–Sutcliffe Efficiency (NSE) and Kling–Gupta Efficiency (KGE) metrics, comparing simulated discharge against observed values. For spatial pattern accuracy, we calculate the Pearson correlation coefficient and Root Mean Square Error (RMSE) between estimated and observed soil moisture values.

The computational complexity of our framework is a key consideration for its application in large-scale hydrological forecasting. To quantify its performance, we provide details on the training process and resource utilization.

- Hardware: All models were trained using 8 cores on an AMD EPYC 7643.
- Mesh Resolution: The computational mesh contains about 25,000 cells.
- Training Duration: Each model was trained for 350 iterations.
- Memory Consumption:
  - HDA-PR & CDC without SM use about 53 GB RAM.
  - HDA-PR & CDC with SM RMSE use about 66 GB RAM.
  - HDA-PR & CDC with SM SP use about 90 GB RAM.
- Iteration times:
  - HDA-PR without SM takes about 990 s per iteration.
  - CDC without SM takes about 900 s per iteration.
  - HDA-PR with SM RMSE takes about 1200 s per iteration.
  - CDC with SM RMSE takes about 1050 s per iteration.
  - HDA-PR with SM SP takes about 3600 s per iteration.
  - CDC with SM SP takes about 3400 s per iteration.
- Forward Simulation Time: Once calibrated, the model's forward computation time is negligible, taking less than 30 s.

For example, HDA-PR with SM SP requires approximately two weeks to complete the full calibration process.

The computational demand of our framework depends on spatial resolution and assimilation frequency. While larger-scale applications require substantial computational resources, efficiency can be enhanced through parallelization techniques. To address these challenges, we are finalizing a new version of this framework, written entirely in Python and utilizing PyTorch for CUDA parallelization. This next-generation version achieves 10×speedups and scales effectively with available hardware resources. While beyond the scope of this study, these improvements will be detailed in a forthcoming GMD article. These advancements will significantly enhance the framework's feasibility for large-scale hydrological forecasting applications, ensuring a balance between computational efficiency and model accuracy.

6. Result analysis

In this section, we analyze the numerical results obtained from our experiments to evaluate the effectiveness of soil moisture data assimilation in hydrological modeling. The analysis is structured to provide a comprehensive overview of the model's performance across different conditions and calibration strategies. We begin by examining the global performance metrics of each models. This initial assessment provides insight into the overall accuracy and reliability of the models when incorporating soil moisture data compared to using traditional streamflow observations alone.

Following the global performance evaluation, we perform a more detailed performance analysis categorized by specific flow ranges and aridity indices. This breakdown allows us to explore how different hydrological conditions ranging from low to high flow and varying degrees of aridity affect the model's predictive capabilities. This step is crucial for understanding the impacts of soil moisture assimilation on model accuracy under diverse hydrological scenarios.

Subsequently, we analyze the correlation between observed and simulated soil moisture to assess the effectiveness of moisture as a calibration objective. This analysis examines whether including soil moisture as a secondary calibration objective enhances model performance or introduces additional complexities. Finally, we evaluate the spatial distribution and characteristics of the calibrated parameters to understand how the assimilation of soil moisture data influences parameter estimation and regionalization within the hydrological model. This comprehensive approach provides a detailed understanding of the strengths and limitations of using soil moisture data assimilation for improving hydrological predictions.

6.1. Discharge performance analysis

In this section, we present and analyze the results of our experiments, focusing on the performance of different models in both spatial and temporal calibration and validation periods. The models evaluated are the HDA-PR model and the CDC model, each tested with three different approaches for incorporating soil moisture data: none, RMSE (root mean square error), and SP (spatial bias insensitive).

Global performances at calibration and validation periods and gauges are presented in terms of NSE in Fig. 3 and of KGE in Fig. 4. The graphs display the NSE and KGE scores of the six models, with results split into calibration (left graph) and validation (right graph) periods, each graph is split into gauged (spatial calibration) and ungauged (spatial validation) subgroups, the ungauged group are the catchments that we hide during calibration in order to assess the regionalization capabilities of each model. Each model's performance is shown through boxplots, where the height of the box represents the interquartile range (IQR), with the median NSE score indicated by a horizontal line inside the box. The whiskers extending from the box show the range of NSE scores, providing insight into the variability and consistency of each model's performance across both periods. The non-hatched group corresponds to the classical distributed calibration without physical descriptors, while the hatched group represents distributed calibration with regionalization using physical descriptors.

The boxplots in Fig. 3 provide a visual comparison of each model's spatio-temporal performances in discharge time series simulation, both at calibration and validation gauges. During the temporal calibration period for spatial calibration (gauged), the HDA-PR models achieve NSE scores ranging from approximately 0.48 to 0.96, with the HDA-PR model calibrated using soil moisture with SP demonstrating more stability and the highest performance with a median NSE of about 0.74. CDC models show no improvement with RMSE incorporation. During spatio-temporal validation, which is the most important for us from an operational perspective (for forecasting and use in ungauged areas), is where the results show the most significant impact of incorporating soil moisture (SM), the reduced variability in the performance of the

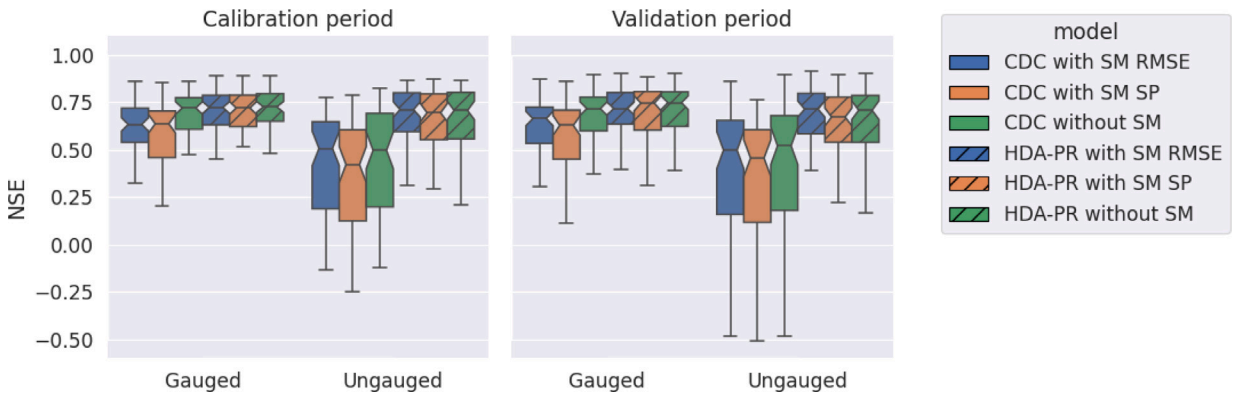

Fig. 3. The Nash–Sutcliffe Efficiency (NSE) scores for the six models during both the calibration and validation periods (left and right graphs), broken down into spatial and temporal analyses.

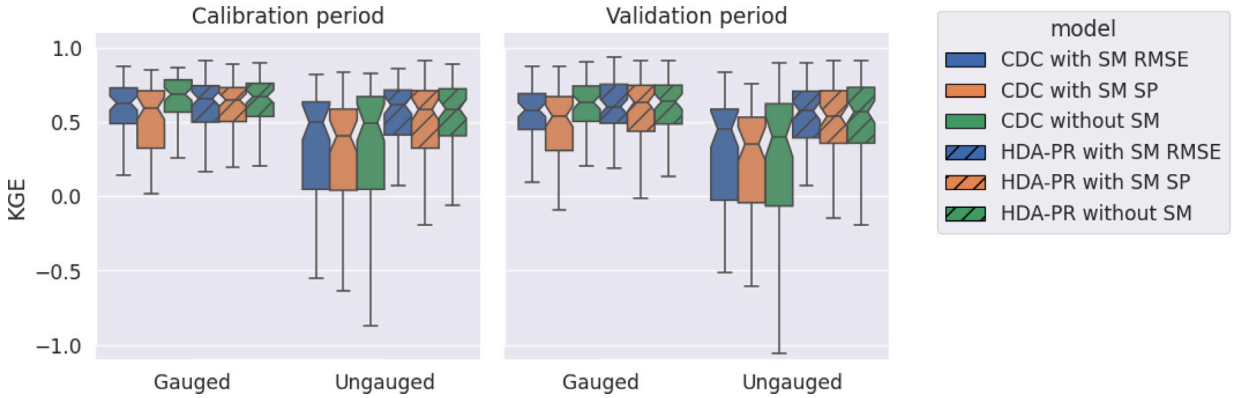

Fig. 4. The Kling–Gupta Efficiency (KGE) scores for the six models during both the calibration and validation periods, broken down into spatial and temporal analyses.

HDA-PR model with soil moisture assimilation is also observed here with the RMSE approach yielding the most stable and highest NSE scores for both HDA-PR and CDC models. This demonstrates the value of soil moisture data in improving the regionalization capabilities of the hydrological model. The HDA-PR models, benefit significantly from soil moisture integration, especially through the RMSE calibration, which consistently outperforms other approaches.

Discharge modeling performances in terms of KGE are presented in Fig. 4. Over the calibration period, for ungauged catchments (spatial validation), the HDA-PR with SM RMSE model achieves the highest stability and performance compared to other methods, especially the regionalization HDA-PR without SM. In spatio-temporal validation, i.e. on validation period and on ungauged catchments, the HDA-PR with SM RMSE model demonstrates reduced performance variability and maintains a high median KGE score of around 0.70. This consistent performance across periods highlights the effectiveness of incorporating spatio-temporal soil moisture data with RMSE cost function, enhancing both the accuracy and stability of the models. The CDC models show moderate improvement with soil moisture, but the HDA-PR models, particularly with RMSE integration, exhibit the most reliable and stable performance.

The Nash–Sutcliffe Efficiency (NSE) scores for the six models during spatio-temporal validation are shown in Fig. 5. These models are grouped based on catchment mean hourly discharge ranges: < 5, 5–10, 10–15, 15-20, and > 20 cubic meters per second (m^3/s). The performance of models incorporating soil moisture data assimilation (SM-DA) varies across different flow ranges due to differences in dominant hydrological processes. At low flows (0–10 m^3/s), baseflow and groundwater contributions are the primary drivers of streamflow (Beven, 2001). However, since SM-DA constrains surface moisture states, it may lead to slight reductions in discharge performance in catchments where groundwater storage dynamics play a more dominant role (McMillan et al., 2012). This could explain why the CDC model without SM data performs slightly better than its SM-DA counterpart in this flow range, as the additional constraints from soil moisture assimilation may not perfectly align with subsurface processes. Furthermore, the spatial resolution of SMAP L4 data (9 km) may not fully capture fine-scale soil moisture variability in small basins, introducing potential discrepancies that affect discharge predictions (Liu et al., 2024). Alternatively, the HDA-PR with SM RMSE model exhibits higher and more consistent NSE scores. For the 10–15 m^3/s range, the models maintain high NSE scores with minimal differences between those incorporating soil moisture data and those that do not. This suggests that for this range, the model's inherent capability is strong enough to produce accurate results without additional soil moisture data. At higher flows (> 15 m^3/s), both HDA-PR and CDC models maintain high NSE scores. However, the variability in scores is lower for models incorporating SM-DA, suggesting that soil moisture constraints stabilize model performance during extreme flow conditions. This aligns with findings from Massari et al. (2015), which highlight that SM-DA improves peak flow estimation and flood forecasting at high flows. Overall, the HDA-PR model benefits the most from the integration of soil moisture data showing slightly better performance in lower discharge ranges (< 10 m^3/s), indicating that the hybrid data assimilation and parameter regionalization approach may be more effective in these conditions. In higher discharge ranges (> 10 m^3/s), the performance of both HDA-PR and CDC models converges, with soil moisture data having a lesser but still positive impact when calibrating using the spatial bias insensitive metric.

Fig. 6 illustrates the Nash–Sutcliffe Efficiency (NSE) scores for the six models evaluated during spatio-temporal validation, categorized by catchment aridity index (P/PET) ranges: 0.6–1.2, 1.2–1.8, 1.8–2.4, and 2.4–3. In catchments with an aridity index of 0.6–1.2, there is notable

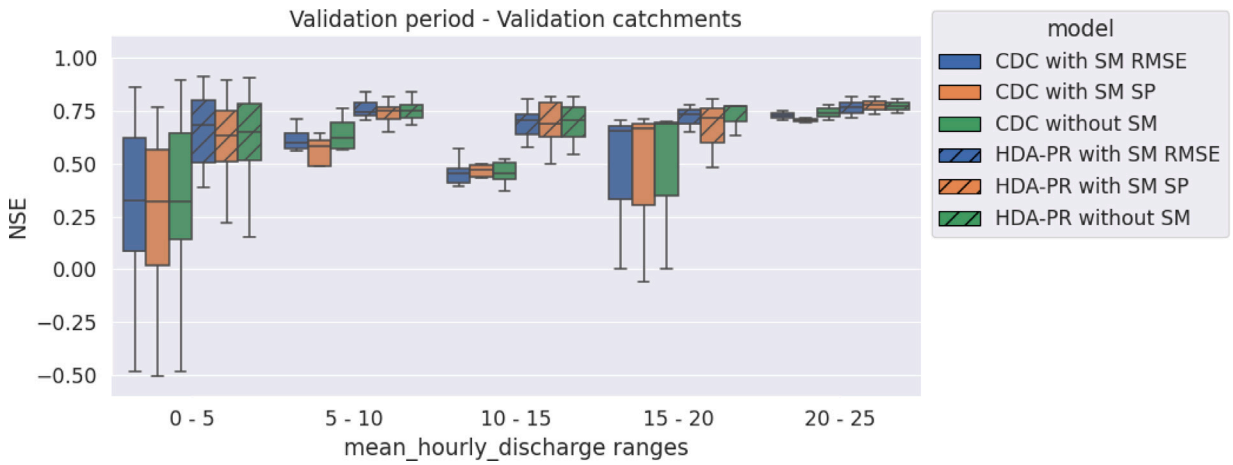

Fig. 5. The Nash–Sutcliffe Efficiency (NSE) scores for the six models during spatio-temporal validation, grouped by catchment mean hourly discharge ranges (m^3/s).

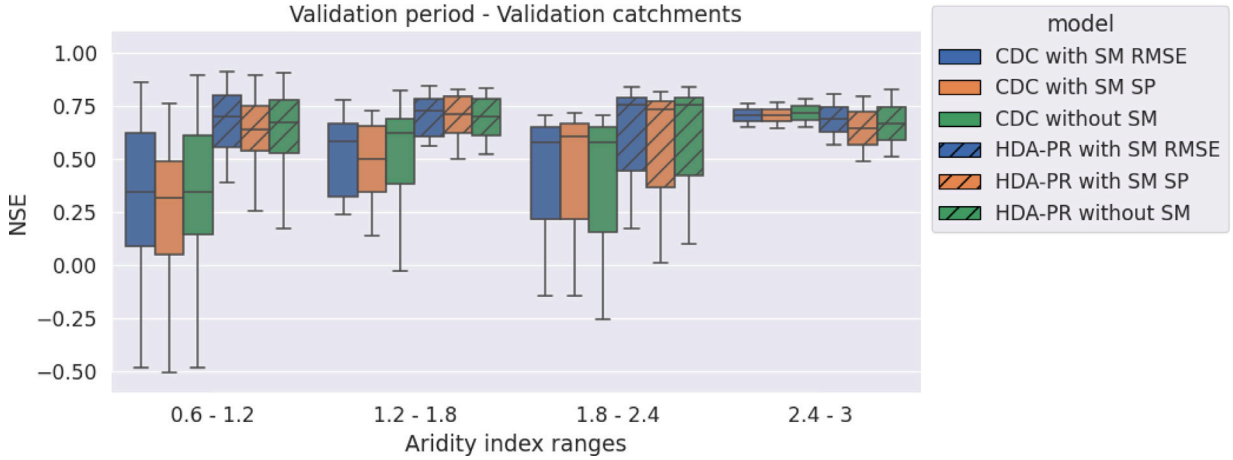

Fig. 6. The Nash–Sutcliffe Efficiency (NSE) scores for the six models during spatio-temporal validation, grouped by catchment aridity index (P/PET) ranges.

variability in NSE scores, particularly for models without soil moisture (SM) data, whereas models integrating SM data, such as "HDA-PR with SM RMSE" and "CDC with SM RMSE," demonstrate higher and more consistent NSE values. Within the 1.2–1.8 aridity index range, the models display higher and more stable NSE scores, with the inclusion of SM data (both RMSE and SP methods) reducing variability and enhancing median NSE scores. In the 1.8–2.4 aridity index range, the models maintain high NSE scores with minimal differences between those incorporating SM data and those without, indicating sufficient model accuracy in moderately arid conditions without additional SM data. In the 2.4–3 aridity index range, while models continue to show high NSE scores, variability is somewhat higher for models without SM data, though less pronounced compared to lower aridity ranges, suggesting reduced dependence on SM data in more wet conditions. Incorporating SM data with RMSE generally improves the regionalization's model performances, more so in very dry and very wet conditions (aridity of 0.6–1.2 and 2.4–3), indicating the added value of SM data calibration using RMSE on the hybrid data assimilation and parameter regionalization approach under extreme meteorological conditions.

6.2. Coherence between observed and simulated moisture

The provided graphs in Fig. 7 illustrate the difference in Pearson correlation coefficients (PCC) between observed soil moisture and modeled soil moisture from two models, CDC and HDA-PR, using two different calibration methods: RMSE and SP. The calculation of the Pearson correlation coefficient (PCC) difference between observed and modeled soil moisture (SM) involves several steps. Initially, for each of our configurations, we determine the PCC on a pixel-by-pixel basis between the observed soil moisture data from SMAP-L4 and the modeled soil moisture from the state of the production reservoir. This step is performed for models both with and without soil moisture calibration. Next, we calculate the difference in the correlation coefficients obtained from the two models (with and without soil moisture calibration) for each pixel. This difference highlights the impact of soil moisture calibration by indicating how much the correlation with observed data improves when calibration is included, thus allowing for a detailed spatial analysis of the impact of soil moisture calibration on model accuracy. For the CDC model, both calibration methods (RMSE and SP) show substantial impacts on PCC differences, with a wider range of values (−0.6 to 0.6). The regions highlighted in red indicate areas where calibration significantly improves the correlation between modeled and observed soil moisture, demonstrating the added value of incorporating soil moisture data. In contrast, blue regions indicate areas where calibration has decreased the correlation, suggesting variability in calibration effectiveness across different areas. SP calibration, in particular, exhibits a more varied impact with notable improvements in several regions. For the HDA-PR model, the calibration effects are more localized, with PCC differences ranging from −0.15 to 0.15. This indicates that while soil moisture calibration still influences model performance, its impact is less pronounced compared to the CDC model. Both RMSE and SP calibration methods show similar patterns of improvement and reduction in correlation across different regions. The narrower range of PCC differences suggests that the HDA-PR model's performance is less sensitive to soil moisture calibration,

Fig. 7. Difference in Pearson Correlation Coefficient Between Observed (SMAP-L4) and Modeled Soil Moisture: Spatial evaluation of the impact of calibration with soil Moisture maps in addition to multi-site discharge, red indicates a gain in correlation, blue indicates a loss, and zero is represented as white. Spatial coordinates are in Lambert 93 and graph scales in km. (For interpretation of the references to color in this figure legend, the reader is referred to the web version of this article.)

but the method still enhances regionalization performances in terms of correlation to observed moisture in most areas. Indeed SMASH with the classical spatially distributed calibration is less constrained than HDA-PR which leverages physical descriptor maps. In HDA-PR, other spatially distributed data, such as these descriptors, act as a strong constraint in the forward model, while soil moisture is used in the objective function, serving as a weak constraint in the optimization problem. This interplay between strong and weak constraints shapes the spatial distribution of the inferred parameters, which we now explore in detail through the analysis of the parameter maps.

6.3. Inferred hydrological parameter maps

We first present spatial maps of calibrated parameters, masked on the basins of interest, to qualitatively analyze the spatial variability of each parameter obtained with HDA-PR, with and without moisture data. The different functioning points reached in the space of conceptual parameters θ for the different optimization experiments are then analyzed.

Fig. 8 shows the inferred hydrological parameter maps for the HDA-PR model, comparing the calibration with soil moisture using RMSE and SP methods, and without soil moisture calibration. Each row represents different hydrological parameters: capacity of the production reservoir, capacity of the transfer reservoir, non-conservative water exchange flux, and the linear routing parameter. For the capacity of the production reservoir maps, both models with SM RMSE and without SM calibration methods show similar spatial patterns, with HDA-PR with SM RMSE showing higher variability, especially in the south-west and central regions, these are the same regions showing a higher correlation between observed and simulated soil moisture in Fig. 6, indicating that soil moisture data influence the estimation of the production reservoir's capacity. The map with soil moisture calibration using SP shows a broader distribution of higher fluxes, suggesting that the spatial bias insensitive metric produces a finer spatial variability of the production reservoir's capacity. The same conclusions as before can be drawn for the capacity of the transfer reservoir with the HDA-PR model using RMSE and without soil moisture calibration; however, the SP model shows less variability than before. This suggests that the transfer reservoir compensates for the production reservoir's capacity to minimize the error in terms of calibration cost function, thereby demonstrating a complementary role in the hydrological balance dynamics. The third row of Fig. 8 displays maps of the non-conservative water exchange parameter that controls the flux of water that is not conserved within the system, indicating areas where water is either gained or lost, supposedly to account for groundwater interactions, and helps here to compensate data and modeling uncertainties and better fit discharge and moisture data (cf. inverse problem (14)). In the maps calibrated with RMSE and without SM vs SP methods, there are notable differences in the spatial distribution of the water exchange parameter, the RMSE calibration and the calibration without SM show a higher and more generalized pattern, particularly concentrated in the northern and southern regions, indicated by yellow and blue areas. These high flux areas suggest regions with significant water exchange determined through the calibration process that aims to fit discharge only or

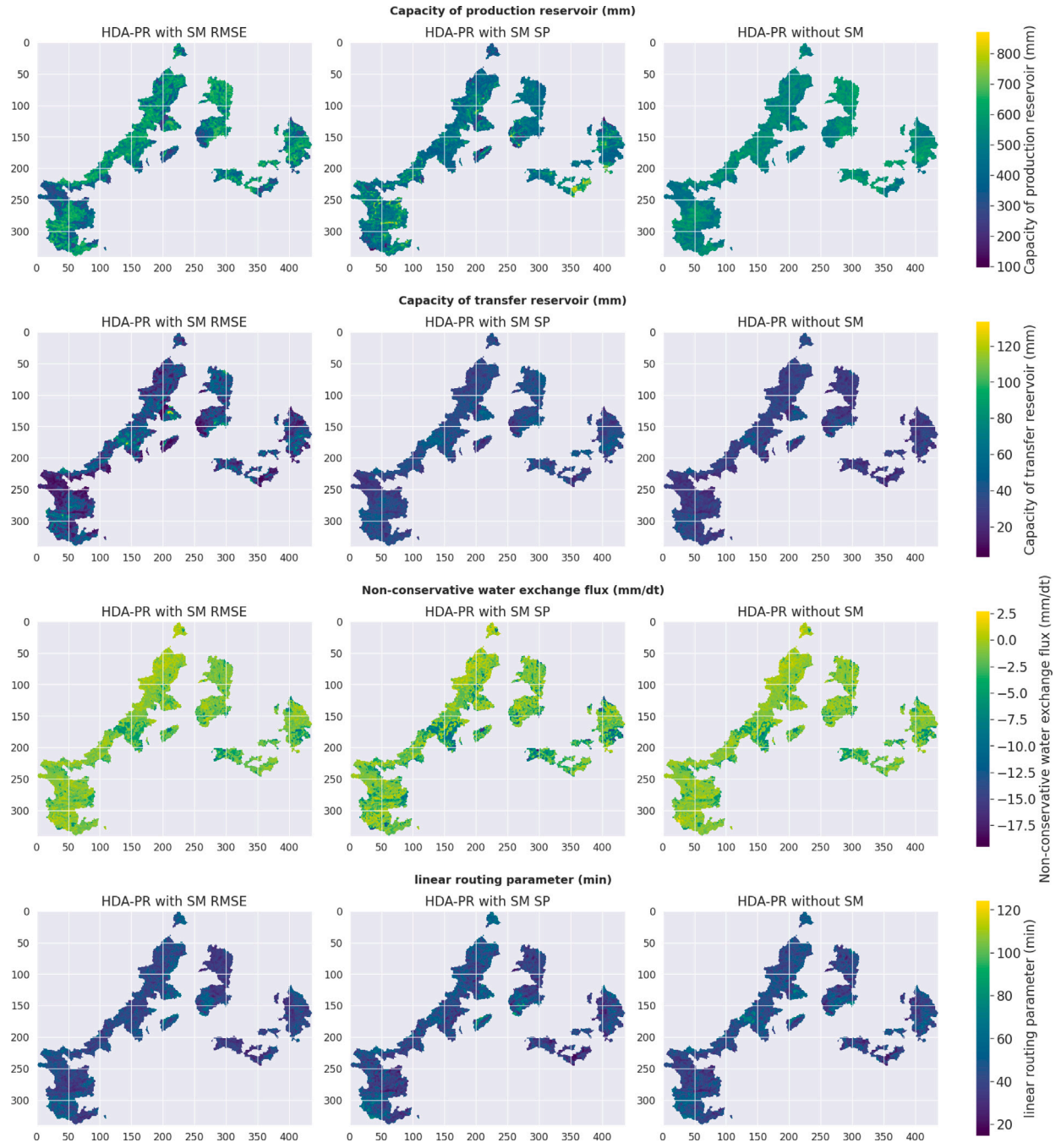

Fig. 8. Inferred Hydrological Parameter $\theta(x)$ Maps with HDA-PR Model: Calibration with Soil Moisture (RMSE & SP) vs. Without Soil Moisture Calibration. Spatial coordinates are in Lambert 93 and graph scales in km.

discharge and moisture maps. In contrast, the SP calibration method displays a more varied and detailed spatial distribution, with high flux regions still present but more dispersed. The final row shows the linear routing parameter. The three calibration methods yield similar spatial patterns indicating that soil moisture data does not impact the estimation of the routing parameter. Spatial statistics resulting from the inferred parameter maps, using various calibration strategies, are presented in the appendix. The footprint of physical descriptors maps accounted for in HDA-PR is analyzed after.

Fig. 9(c) examines the linear correlation between the various physical descriptors assimilated in the HDA-PR model and its hydrological parameters under different calibration conditions: "With SM RMSE," "With SM SP," and "Without SM." The physical descriptors considered are slope (d_1), drainage density (d_2), percentage in karst (d_3), forest cover rate (d_4), urban cover rate (d_5), potential water reserve (d_6), and high storage capacity rate (d_7). The hydrological parameters analyzed include the capacity of the production reservoir (C_p), the capacity of the transfer reservoir (C_t), the non-conservative water exchange flux (k_{exc}), and the linear routing parameter (lr).

Under the calibration with RMSE, the highest correlation is observed between the forest cover rate (d_4) and the capacity of the production reservoir (C_p). This indicates that areas with higher forest cover significantly impact water storage when considering Soil Moisture with RMSE. Additionally, the drainage density (d_2) and forest cover rate (d_4) show a moderate correlation with the capacity of the transfer reservoir (C_t), suggesting that karst regions and forest areas influence the transfer capacity. Also, the urban cover rate (d_5) shows a moderate correlation with the water exchange flux (k_{exc}). Other

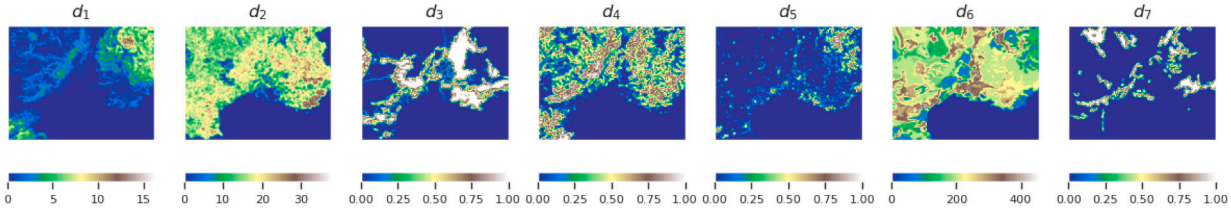

(a) Spatial distribution of physical descriptors: d_1: Slope, d_2: Drainage density, d_3: % in karst, d_4: Forest cover rate, d_5 Urban cover rate, d_6: Potential water reserve, d_7: High storage capacity rate.

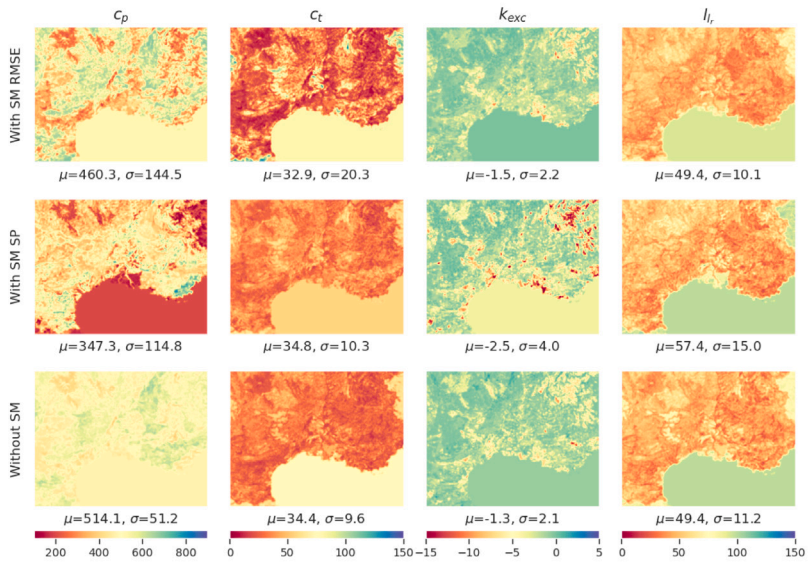

(b) Spatial distribution of calibrated hydrological parameters with μ and σ indicating their spatial average and standard deviation over the active cells within the spatial domain Ω

(c) Linear correlation between descriptors and parameters over the active cells within the spatial domain Ω

Fig. 9. Analysis of input descriptors and inferred model parameters for the regionalization method (HDA-PR) across the three soil moisture calibration setups (With SM RMSE, With SM SP, and Without SM).

descriptors, such as slope (d_1), potential water reserve (d_6) and high storage capacity rate (d_7), do not show correlations with hydrological parameters.

In soil moisture calibration using the spatial bias-insensitive metric, the transfer reservoir (C_t) and the water exchange flux (k_{exc}) have the same correlations as RMSE calibration. However, the capacity of the production reservoir (C_p) and the linear routing parameter (lr) are more correlated with the drainage density, indicating that the drainage density has a stronger impact on the parameters under SM SP calibration. Other descriptors, such as slope (d_1), potential water reserve (d_6), and high storage capacity rate (d_7), do not show correlations with hydrological parameters.

Without considering Soil Moisture, the slope (d_1), the potential water reserve (d_6), and the high storage capacity rate (d_7) show no correlations with the hydrological parameters same as with SM calibration, indicating that none of the calibration methods was improved by using these descriptors. The transfer reservoir parameter (C_t) and the linear routing parameter (lr) show moderate correlations with drainage density (d_2). The capacity of production (C_p) is more correlated to the % in karst (d_3) and the forest cover rate (d_4) suggesting that these features influence the production reservoirs even without considering soil moisture.

The one-to-one correspondence between parameters and descriptors, visualized in correlation matrices, enhances the interpretability of the calibrated regionalization ANN by revealing how the ANN leverages descriptor map information to inform the conceptual model parameters. The physical relevance of the inferred spatial distribution of parameters is demonstrated by discharge modeling accuracy at available gauges and by correlations obtained between simulated and observed moisture. These results underscore the value of the inferred spatial parameter distributions, which represent optimal solutions of the inverse problem (14). These solutions integrate information from two sources: (1) physical descriptors utilized by the NN embedded as strong constrain into the conceptual model, and (2) discharge and moisture observations. The latter, representing partial observations of real-world hydrological responses, serve as weak constraints within the assimilation's cost function. A more in-depth physical analysis could be achieved with a physically based model structure and soil data that could be integrated in the proposed framework in future research.

7. Discussions

The primary objective of this study was to assess the efficacy of integrating satellite-derived soil moisture data with traditional streamflow observations for improving the parameter regionalization and the performances of a spatially distributed hydrological model in simulating both discharge and surface moisture. The study used the hybrid data assimilation and parameter regionalization (HDA-PR) approach from Huynh et al. (2024), which integrates neural networks into the differentiable spatially distributed hydrological model SMASH.

The results demonstrated that the inclusion of satellite soil moisture data significantly enhances the model's ability to predict both soil moisture and discharge. This improvement was evident across various metrics used to evaluate model performance. Specifically, the regional optimizations performed on flash-flood-prone areas in Southern France

showed enhanced accuracy and robustness in simulated discharge and soil moisture when compared to traditional methods that only used streamflow measurements. The improvement in model performance can be attributed to the additional information provided by the satellite-derived soil moisture data, which is spatially distributed and covers both gauged and ungauged basins, which helps to better constrain the model. This leads to more accurate simulations in terms of discharge and spatio-temporal moisture as testified by the good correlation/fit to the available data. The integration of this data helps to mitigate some of the uncertainties inherent in hydrological modeling, particularly in areas with heterogeneous climatic and physiographic conditions. The findings align with previous research that has demonstrated the benefits of using remote sensing data for hydrological model calibration and validation. For instance, studies by Li et al. (2023), Wanders et al. (2014), Chao et al. (2022) have shown that the incorporation of multiple variables such as soil moisture and water storage data from remote sensing can enhance hydrological model performance. This study extends these findings by demonstrating the effectiveness of a variational data assimilation (VDA) method in a high-resolution conceptual hydrological model with descriptors-based regionalization.

Despite the positive outcomes, there are some limitations to the study. One significant limitation is the assumption of unbiased Gaussian uncertainties in the variational data assimilation framework. This assumption might not hold true in all cases, potentially affecting the robustness of the results. Additionally, the study focused on a specific region in Southern France, and the applicability of the findings to other regions with different hydrological characteristics remains to be explored with the proposed method that is transposable.

Future research should aim to validate the findings of this study in other regions and under different climatic conditions. Additionally, further work is needed to refine the data assimilation framework to account for non-Gaussian uncertainties and to explore the integration of other types of remote sensing data, such as evaporation and land use. Expanding the study to include a broader range of hydrological models, including physically based soil-vegetation models, and assimilation algorithms could also provide deeper insights into the generalizability and robustness of the HDA-PR approach.

Overall, the integration of satellite-derived soil moisture data into a distributed hydrological model using a VDA approach shows considerable promise for improving model accuracy and reliability. This study provides a solid foundation for further exploration and development of advanced data assimilation techniques in hydrological modeling with classical model structures as done here of with hybrid physical-ML ones.

8. Conclusion

This study has demonstrated the significant potential of integrating satellite-derived soil moisture data with streamflow observations to enhance the performance of distributed hydrological models at gauged and ungauged sites. By employing a Hybrid Data Assimilation and Parameter Regionalization (HDA-PR) approach within the differentiable hydrological model SMASH, we achieved substantial improvements in the accuracy and robustness of simulated discharge and soil moisture, particularly in flash-flood-prone areas of Southern France. The inclusion of satellite soil moisture data provided additional constraints on the model, reducing uncertainties and leading to more precise simulations of hydrological processes. These findings are consistent with previous research, reinforcing the value of remote sensing data in hydrological model calibration and validation using hybrid approaches.

We can draw the following conclusions from calibration on both multi-site discharge time series and soil moisture maps:

- Overall better spatio-temporal performances of discharge and soil moisture estimation.
- Significant added value for both extremely dry and extremely wet conditions.
- Significant added value for small catchments, particularly those with low mean hourly discharge.

However, this study also highlighted certain limitations, such as the assumption of unbiased Gaussian uncertainties in the Bayesian framework and the focus on a specific geographical region. Future research should aim to address these limitations by testing the approach in diverse climatic and physiographic contexts, refining the data assimilation framework, and incorporating a broader range of remote sensing data. In summary, the integration of satellite-derived soil moisture data using a variational data assimilation (VDA) in a hybrid regionalization method shows great promise for improving hydrological modeling. This research provides a robust foundation for future studies aiming to enhance the accuracy and reliability of hydrological predictions through advanced gradient-based data assimilation techniques. The findings underscore the importance of leveraging remote sensing technologies to better understand and manage water resources, particularly in regions vulnerable to extreme hydrological events.

CRediT authorship contribution statement

Mouad Ettalbi: Writing – original draft, Visualization, Validation, Software, Methodology, Formal analysis, Data curation, Conceptualization. **Pierre-André Garambois:** Writing – review & editing, Validation, Supervision, Resources, Project administration, Methodology, Funding acquisition, Conceptualization. **Ngo-Nghi-Truyen Huynh:** Writing – review & editing. **Patrick Arnaud:** Writing – review & editing. **Emmanuel Ferreira:** Writing – review & editing. **Nicolas Baghdadi:** Writing – review & editing.

Code availability

The SMASH source code and the scripts used for conducting the numerical experiments and analysis in this study are available at: https://github.com/DassHydro-dev/smash. The data supporting this study will be made available by the corresponding author upon reasonable request.

Declaration of competing interest

The authors declare the following financial interests/personal relationships which may be considered as potential competing interests: Mouad ETTALBI reports financial support was provided by National Association of Technical Research. If there are other authors, they declare that they have no known competing financial interests or personal relationships that could have appeared to influence the work reported in this paper.

Acknowledgment

The ANRT (French national association for research and technology) is acknowledged for financial support of CIFRE PhD of the first author with Aiway compagny.

Appendix. Spatial statistics of inferred parameter maps

To provide a more quantitative view of the spatial parameter maps, Fig. 10 presents a spatial statistical analysis of the inferred hydrological parameters over the catchments sample. The figure is structured such that the columns represent the calibrated hydrological parameters, and the rows represent the statistical measures, each model's parameter statistic is shown through a violin plot. A violin plot displays the distribution of the data, showing both the density and the range of values for each parameter. The width of the plot at any given value indicates the

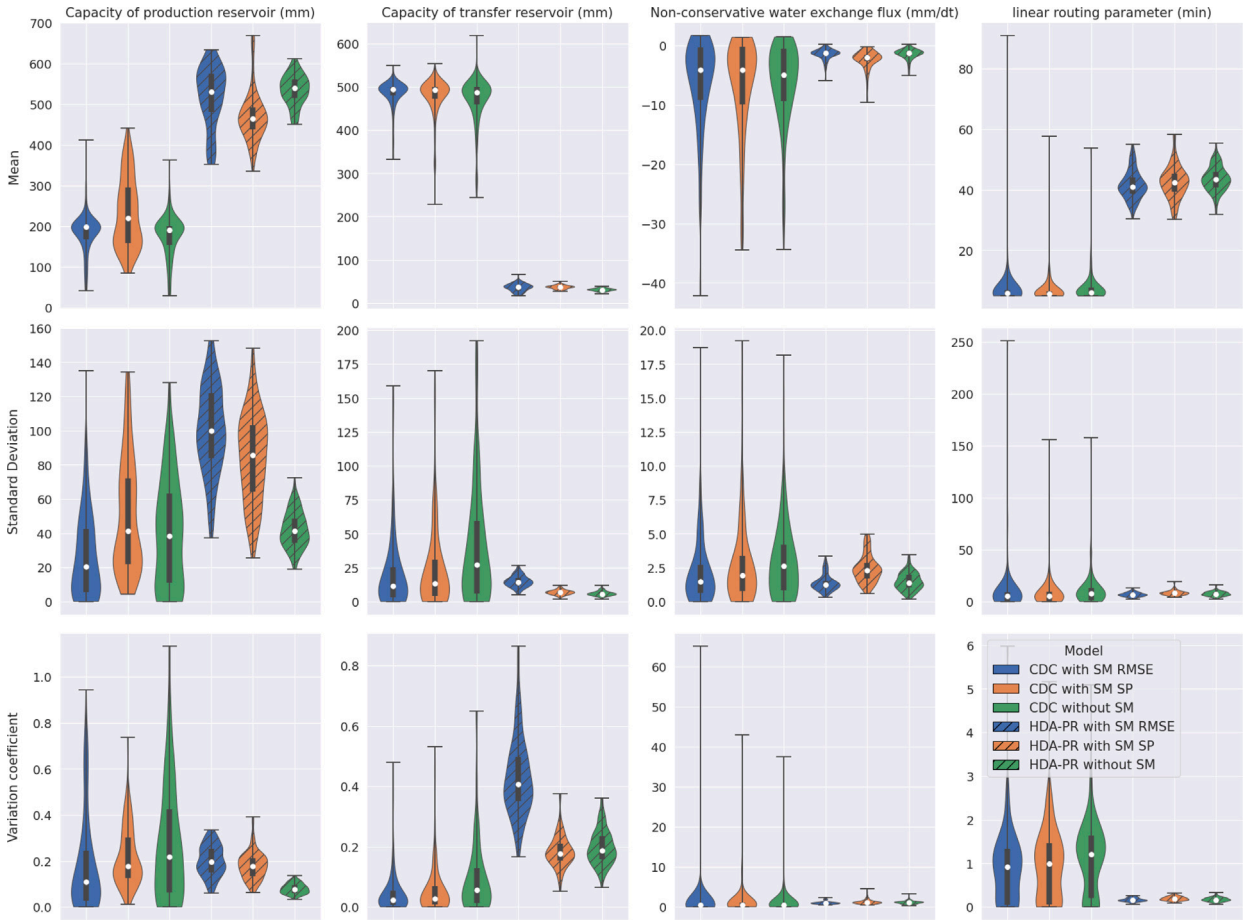

Fig. 10. Spatial statistical analysis of inferred Hydrological Parameters per catchment: columns represent the calibrated hydrological parameters and rows represent the statistic measure.

frequency of data points at that level, with a thicker section representing more data points and a thinner section representing fewer, while the white dot represents the median value. Additionally, the shape of the plot can provide insight into the skewness (asymmetry) and kurtosis (peakedness) of the distribution, with wider tails suggesting higher kurtosis and asymmetrical shapes indicating skewness and the presence of outliers.

The mean values of C_p show that soil moisture calibration methods (RMSE and SP) significantly influence the spatial distribution of this parameter. For the HDA-PR model, the standard deviation is higher for RMSE than for SP, suggesting greater variability in the production reservoir capacity when the RMSE calibration. Skewness and kurtosis values indicate that the distribution of C_p is more skewed and has heavier tails for RMSE, suggesting more extreme values compared to SP. For the CDC model, RMSE calibration has the opposite effect on C_p variability showing the least standard deviation. However, the spatial bias insensitive (SP) calibration method produces more variability, suggesting a refined estimation process. Similarly to C_p, the capacity of the transfer reservoir (C_t) the mean values show distinct spatial patterns influenced by the calibration methods, the standard deviation for C_t is also higher for RMSE, indicating more variability. The skewness and kurtosis values follow a similar trend to C_p, with RMSE showing more skewed and leptokurtic distributions for the HDA-PR model. This indicates a complementary role between the production and transfer reservoirs, where adjustments in one parameter may balance out discrepancies into another to maintain overall hydrological balance. The non-conservative water exchange flux (k_{exc}) statistics indicate that calibration with SP results in a more balanced spatial distribution of k_{exc}. SP calibration shows higher variability (standard deviation) and more extreme values (skewness and kurtosis), indicating that this method might introduce more significant discrepancies in the flux values of the HDA-PR model. The mean values for the linear routing parameter (lr) are relatively similar across calibration methods, suggesting that soil moisture data calibration in addition to multi-gauge discharge has a limited impact on this parameter.

The analysis of Fig. 10 underscores the critical role of calibration methods in influencing the spatial distribution and statistical properties of hydrological parameters. The RMSE calibration tends to introduce more variability and extreme values, especially for parameters like C_p and C_t. In contrast, the SP calibration method provides a more balanced and stable distribution.

Data availability

Data will be made available on request.

References

Alfieri, L., Avanzi, F., Delogu, F., Gabellani, S., Bruno, G., Campo, L., Libertino, A., Massari, C., Tarpanelli, A., Rains, D., Miralles, D.G., Quast, R., Vreugdenhil, M., Wu, H., Brocca, L., 2022. High-resolution satellite products improve hydrological modeling in northern Italy. Hydrol. Earth Syst. Sci. 26 (14), 3921–3939.

Baghdadi, N., Bernier, M., Neeson, I., 2001. Evaluation of C-band SAR data for wetlands mapping. Int. J. Remote Sens. 22 (1), 71–88. http://dx.doi.org/10.1080/014311601750038857.

Bechtold, M., Modanesi, S., Lievens, H., Baguis, P., Brangers, I., Carrassi, A., Getirana, A., Gruber, A., Heyvaert, Z., Massari, C., Scherrer, S., Vannitsem, S., De Lannoy, G., 2023. Assimilation of sentinel-1 backscatter into a land surface model with river routing and its impact on streamflow simulations in two belgian catchments. J. Hydrometeorol. 24 (12), 2389–2408.

Beven, K., 1987. Towards a new paradigm in hydrology. IAHS Publication.
Beven, K., 2001. Rainfall-Runoff Modelling: The Primer. Wiley.
Bou-Fakhreddine, B., Mougharbel, I., Faye, A., Abou Chakra, S., Pollet, Y., 2018. Daily river flow prediction based on two-phase constructive fuzzy systems modeling: A case of hydrological – meteorological measurements asymmetry. J. Hydrol. (Amsterdam) 558, 255–265.
Brocca, L., Zhao, W., Lu, H., 2023. High resolution observations from space to address new applications in hydrology. Innov. 4, 100437. http://dx.doi.org/10.1016/j.xinn.2023.100437.
Castelli, F., 2023. Data assimilation in hydrological sciences. In: Ismail-Zadeh, A., Castelli, F., Jones, D., Sanchez, S. (Eds.), Applications of Data Assimilation and Inverse Problems in the Earth Sciences. In: Special Publications of the International Union of Geodesy and Geophysics, Cambridge University Press, pp. 112–130.
Cenci, L., Pulvirenti, L., Boni, G., Chini, M., Matgen, P., Gabellani, S., Squicciarino, G., Pierdicca, N., 2017. An evaluation of the potential of sentinel 1 for improving flash flood predictions via soil moisture–data assimilation. Adv. Geosci. 44, 89–100.
Chao, L., Zhang, K., Wang, S., Gu, Z., Xu, J., Bao, H., 2022. Assimilation of surface soil moisture jointly retrieved by multiple microwave satellites into the WRF-hydro model in ungauged regions: Towards a robust flood simulation and forecasting. Environ. Model. Softw. : With Environ. Data News 154, 105421.
Dembélé, M., Hrachowitz, M., Savenije, H.H.G., Mariéthoz, G., Schaefli, B., 2020. Improving the predictive skill of a distributed hydrological model by calibration on spatial patterns with multiple satellite data sets. Water Resour. Res. 56 (1), e2019WR026085. http://dx.doi.org/10.1029/2019WR026085, arXiv:https://agupubs.onlinelibrary.wiley.com/doi/pdf/10.1029/2019WR026085, URL https://agupubs.onlinelibrary.wiley.com/doi/abs/10.1029/2019WR026085, e2019WR026085 2019WR026085.
Demirel, M.C., Mai, J., Mendiguren, G., Koch, J., Samaniego, L., Stisen, S., 2018. Combining satellite data and appropriate objective functions for improved spatial pattern performance of a distributed hydrologic model. Hydrol. Earth Syst. Sci. 22 (2), 1299–1315. http://dx.doi.org/10.5194/hess-22-1299-2018, URL https://hess.copernicus.org/articles/22/1299/2018/.
Ding, Z., Lü, H., Ahmed, N., Zhu, Y., Gou, Q., Wang, X., Liu, E., Xu, H., Pan, Y., Sun, M., 2022. Soil moisture data assimilation in MISDc for improved hydrological simulation in upper huai river basin, China. Water 14 (21), http://dx.doi.org/10.3390/w14213476, URL https://www.mdpi.com/2073-4441/14/21/3476.
El Hajj, M., Baghdadi, N., Zribi, M., Bazzi, H., 2017. Synergic use of sentinel-1 and sentinel-2 images for operational soil moisture mapping at high spatial resolution over agricultural areas. Remote. Sens. 9 (12), http://dx.doi.org/10.3390/rs9121292, URL https://www.mdpi.com/2072-4292/9/12/1292.
Entekhabi, D., Njoku, E.G., O'Neill, P.E., Kellogg, K.H., Crow, W.T., Edelstein, W.N., Entin, J.K., Goodman, S.D., Jackson, T.J., Johnson, J., Kimball, J., Piepmeier, J.R., Koster, R.D., Martin, N., McDonald, K.C., Moghaddam, M., Moran, S., Reichle, R., Shi, J.C., Spencer, M.W., Thurman, S.W., Tsang, L., Van Zyl, J., 2010. The soil moisture active passive (SMAP) mission. Proc. IEEE 98 (5), 704–716. http://dx.doi.org/10.1109/JPROC.2010.2043918.
Ficklin, D.L., Null, S.E., Abatzoglou, J.T., Novick, K.A., Myers, D.T., 2022. Hydrological intensification will increase the complexity of water resource management. Earth' s Futur. 10 (3), n/a.
Fowler, H.J., Wasko, C., Prein, A.F., 2021. Intensification of short-duration rainfall extremes and implications for flood risk: current state of the art and future directions. Philos. Trans. R. Soc. Lond. Ser. A: Math. Phys. Eng. Sci. 379 (2195), 20190541.
Guerreiro, S.B., Fowler, H.J., Barbero, R., Westra, S., Lenderink, G., Blenkinsop, S., Lewis, E., Li, X., 2018. Detection of continental-scale intensification of hourly rainfall extremes. Nat. Clim. Chang. 803–808.
Gupta, H.V., Kling, H., Yilmaz, K.K., Martinez, G.F., 2009. Decomposition of the mean squared error and NSE performance criteria: Implications for improving hydrological modelling. J. Hydrol. 377 (1), 80–91. http://dx.doi.org/10.1016/j.jhydrol.2009.08.003, URL https://www.sciencedirect.com/science/article/pii/S0022169409004843.
Houser, P., Lannoy, G., Walker, J., 2012. Hydrologic data assimilation. ISBN: 978-953-51-0294-6, http://dx.doi.org/10.5772/31246.
Huynh, N.N.T., Garambois, P.-A., Colleoni, F., Renard, B., Roux, H., Demargne, J., Jay-Allemand, M., Javelle, P., 2024. Learning regionalization using accurate spatial cost gradients within a differentiable high-resolution hydrological model: Application to the french mediterranean region. Water Resour. Res. 60 (11), e2024WR037544. http://dx.doi.org/10.1029/2024WR037544, arXiv:https://agupubs.onlinelibrary.wiley.com/doi/pdf/10.1029/2024WR037544, URL https://agupubs.onlinelibrary.wiley.com/doi/abs/10.1029/2024WR037544, e2024WR037544 2024WR037544.
Jadidoleslam, N., Mantilla, R., Krajewski, W.F., 2021. Data assimilation of satellite-based soil moisture into a distributed hydrological model for streamflow predictions. Hydrology 8 (1), 52.
Jay-Allemand, M., Demargne, J., Garambois, P.-A., Javelle, P., Gejadze, I., Colleoni, F., Organde, D., Arnaud, P., Fouchier, C., 2024. Spatially distributed calibration of a hydrological model with variational optimization constrained by physiographic maps for flash flood forecasting in France. Proc. IAHS 385, 281–290. http://dx.doi.org/10.5194/piahs-385-281-2024, URL https://piahs.copernicus.org/articles/385/281/2024/.
Jay-Allemand, M., Javelle, P., Gejadze, I., Arnaud, P., Malaterre, P.-O., Fine, J.-A., Organde, D., 2020. On the potential of variational calibration for a fully distributed hydrological model: application on a mediterranean catchment. Hydrol. Earth Syst. Sci. 24 (11), 5519–5538. http://dx.doi.org/10.5194/hess-24-5519-2020, URL https://hess.copernicus.org/articles/24/5519/2020/.
Kerr, Y., Waldteufel, P., Wigneron, J.-P., Martinuzzi, J., Font, J., Berger, M., 2001. Soil moisture retrieval from space: the soil moisture and ocean salinity (SMOS) mission. IEEE Trans. Geosci. Remote Sens. 39 (8), 1729–1735. http://dx.doi.org/10.1109/36.942551.
Kherazi, F.Z., Sun, D., Sohu, J.M., Junejo, I., Naveed, H.M., Khan, A., Shaikh, S.N., 2024. The role of environmental knowledge, policies and regulations toward water resource management: A mediated-moderation of attitudes, perception, and sustainable consumption patterns. Sustain. Dev. (Bradf. West Yorks. England).
Kim, D.-H., Johnson, J.M., Clarke, K.C., McMillan, H.K., 2024. Untangling the impacts of land cover representation and resampling in distributed hydrological model predictions. Environ. Model. Softw. : With Environ. Data News 172, 105893.
Köhler, J., Kuenzer, C., 2020. Forecasting spatio-temporal dynamics on the land surface using earth observation data—A review. Remote. Sens. 12, 3513. http://dx.doi.org/10.3390/rs12213513.
Koo, H., Iwanaga, T., Croke, B.F., Jakeman, A.J., Yang, J., Wang, H.-H., Sun, X., Lü, G., Li, X., Yue, T., Yuan, W., Liu, X., Chen, M., 2020. Position paper: Sensitivity analysis of spatially distributed environmental models- a pragmatic framework for the exploration of uncertainty sources. Environ. Model. Softw. 134, 104857. http://dx.doi.org/10.1016/j.envsoft.2020.104857, URL https://www.sciencedirect.com/science/article/pii/S1364815220309142.
Krause, P., Boyle, D.P., Bäse, F., 2005. Comparison of different efficiency criteria for hydrological model assessment. Adv. Geosci. 5, 89–97. http://dx.doi.org/10.5194/adgeo-5-89-2005, URL https://adgeo.copernicus.org/articles/5/89/2005/.
Lavers, D.A., Ramos, M.-H., Magnusson, L., Pechlivanidis, I., Klein, B., Prudhomme, C., Arnal, L., Crochemore, L., Van Den Hurk, B., Weerts, A.H., Harrigan, S., Cloke, H.L., Richardson, D.S., Pappenberger, F., 2020. A vision for hydrological prediction. Atmosphere 11 (3), http://dx.doi.org/10.3390/atmos11030237, URL https://www.mdpi.com/2073-4433/11/3/237.
Lawrence, D.M., Fisher, R.A., Koven, C.D., Oleson, K.W., Swenson, S.C., Bonan, G., Collier, N., Ghimire, B., van Kampenhout, L., Kennedy, D., Kluzek, E., Lawrence, P.J., Li, F., Li, H., Lombardozzi, D., Riley, W.J., Sacks, W.J., Shi, M., Vertenstein, M., Wieder, W.R., Xu, C., Ali, A.A., Badger, A.M., Bisht, G., van den Broeke, M., Brunke, M.A., Burns, S.P., Buzan, J., Clark, M., Craig, A., Dahlin, K., Drewniak, B., Fisher, J.B., Flanner, M., Fox, A.M., Gentine, P., Hoffman, F., Keppel-Aleks, G., Knox, R., Kumar, S., Lenaerts, J., Leung, L.R., Lipscomb, W.H., Lu, Y., Pandey, A., Pelletier, J.D., Perket, J., Randerson, J.T., Ricciuto, D.M., Sanderson, B.M., Slater, A., Subin, Z.M., Tang, J., Thomas, R.Q., Val Martin, M., Zeng, X., 2019. The community land model version 5: Description of new features, benchmarking, and impact of forcing uncertainty. J. Adv. Model. Earth Syst. 11 (12), 4245–4287. http://dx.doi.org/10.1029/2018MS001583, arXiv:https://agupubs.onlinelibrary.wiley.com/doi/pdf/10.1029/2018MS001583, URL https://agupubs.onlinelibrary.wiley.com/doi/abs/10.1029/2018MS001583.
Le, M.-h., Nguyen, B.Q., Pham, H.T., Patil, A., Do, H.X., Ramsankaran, R., Bolten, J.D., Lakshmi, V., 2022. Assimilation of SMAP products for improving streamflow simulations over Tropical Climate Region—Is spatial information more important than temporal information? Remote. Sens. (Basel, Switzerland) 14 (7), 1607.
Legates, D.R., McCabe, Jr., G.J., 1999. Evaluating the use of "goodness-of-fit" measures in hydrologic and hydroclimatic model validation. Water Resour. Res. 35 (1), 233–241. http://dx.doi.org/10.1029/1998WR900018, URL https://agupubs.onlinelibrary.wiley.com/doi/abs/10.1029/1998WR900018.
Li, Y., Cong, Z., Yang, D., 2023. Remotely sensed soil moisture assimilation in the distributed hydrological model based on the error subspace transform Kalman filter. Remote. Sens. (Basel, Switzerland) 15 (7), 1852.
Liang, X., Lettenmaier, D.P., Wood, E.F., Burges, S.J., 1994. A simple hydrologically based model of land surface water and energy fluxes for general circulation models. J. Geophys. Res.: Atmospheres 99 (D7), 14415–14428. http://dx.doi.org/10.1029/94JD00483, arXiv:https://agupubs.onlinelibrary.wiley.com/doi/pdf/10.1029/94JD00483, URL https://agupubs.onlinelibrary.wiley.com/doi/abs/10.1029/94JD00483.
Liu, Y., Cui, W., Ling, Z., Fan, X., Dong, J., Luan, C., Wang, R., Wang, W., Liu, Y., 2024. The impact of satellite soil moisture data assimilation on the hydrological modeling of SWAT in a highly disturbed catchment. Remote. Sens. 16 (2), http://dx.doi.org/10.3390/rs16020429, URL https://www.mdpi.com/2072-4292/16/2/429.
Liu, X., Yang, K., Ferreira, V.G., Bai, P., 2022. Hydrologic model calibration with remote sensing data products in global large basins. Water Resour. Res. 58 (12), e2022WR032929. http://dx.doi.org/10.1029/2022WR032929, arXiv:https://agupubs.onlinelibrary.wiley.com/doi/pdf/10.1029/2022WR032929, URL https://agupubs.onlinelibrary.wiley.com/doi/abs/10.1029/2022WR032929, e2022WR032929 2022WR032929.

Marchi, L., Borga, M., Preciso, E., Gaume, E., 2010. Characterisation of selected extreme flash floods in europe and implications for flood risk management. J. Hydrol. 394, 118–133. http://dx.doi.org/10.1016/j.jhydrol.2010.07.017.

Massari, C., Brocca, L., Tarpanelli, A., Moramarco, T., 2015. Data assimilation of satellite soil moisture into rainfall-runoff modelling: A complex recipe? Remote. Sens. 7, 11403–11433. http://dx.doi.org/10.3390/rs70911403.

Massari, C., Camici, S., Ciabatta, L., Brocca, L., 2018. Exploiting satellite-based surface soil moisture for flood forecasting in the mediterranean area: State update versus rainfall correction. Remote. Sens. (Basel, Switzerland) 10 (2), 292.

McCabe, M.F., Rodell, M., Alsdorf, D.E., Miralles, D.G., Uijlenhoet, R., Wagner, W., Lucieer, A., Houborg, R., Verhoest, N.E.C., Franz, T.E., Shi, J., Gao, H., Wood, E.F., 2017. The future of earth observation in hydrology. Hydrol. Earth Syst. Sci. 21 (7), 3879–3914.

Mcmillan, H., Coxon, G., Sikorska-Senoner, A., Westerberg, I., 2022. Impacts of observational uncertainty on analysis and modelling of hydrological processes: Preface. Hydrol. Process. 36, http://dx.doi.org/10.1002/hyp.14481.

McMillan, H., Krueger, T., Freer, J., 2012. Benchmarking observational uncertainties for hydrology: rainfall, river discharge and water quality. Hydrol. Process. 26 (26), 4078–4111. http://dx.doi.org/10.1002/hyp.9384, arXiv:https://onlinelibrary.wiley.com/doi/pdf/10.1002/hyp.9384, URL https://onlinelibrary.wiley.com/doi/abs/10.1002/hyp.9384.

Messina, J., Evans, T., Manson, S., Shortridge, A., Deadman, P., Verburg, P., 2008. Complex systems models and the management of error and uncertainty. J. Land Use Sci. 3, 11–25. http://dx.doi.org/10.1080/17474230802047989.

Meyer Oliveira, A., Fleischmann, A.S., Paiva, R.C.D., 2021. On the contribution of remote sensing-based calibration to model hydrological and hydraulic processes in tropical regions. J. Hydrol. (Amsterdam) 597, 126184.

Niu, G.-Y., Yang, Z.-L., Mitchell, K.E., Chen, F., Ek, M.B., Barlage, M., Kumar, A., Manning, K., Niyogi, D., Rosero, E., Tewari, M., Xia, Y., 2011. The community noah land surface model with multiparameterization options (noah-MP): 1. Model description and evaluation with local-scale measurements. J. Geophys. Res.: Atmospheres 116 (D12), http://dx.doi.org/10.1029/2010JD015139, arXiv:https://agupubs.onlinelibrary.wiley.com/doi/pdf/10.1029/2010JD015139, URL https://agupubs.onlinelibrary.wiley.com/doi/abs/10.1029/2010JD015139.

Odry, J., 2017. Prédétermination des débits de crues extrêmes en sites non jaugés. Régionalisation de la méthode par simulation SHYREG. (Ph.D. thesis). http://dx.doi.org/10.13140/RG.2.2.26248.32009.

Oudin, L., Hervieu, F., Michel, C., Perrin, C., Andréassian, V., Anctil, F., Loumagne, C., 2005. Which potential evapotranspiration input for a lumped rainfall–runoff model?: Part 2—Towards a simple and efficient potential evapotranspiration model for rainfall–runoff modelling. J. Hydrol. 303 (1), 290–306. http://dx.doi.org/10.1016/j.jhydrol.2004.08.026, URL https://www.sciencedirect.com/science/article/pii/S0022169404004056.

Peng, J., Albergel, C., Balenzano, A., Brocca, L., Cartus, O., Cosh, M.H., Crow, W.T., Dabrowska-Zielinska, K., Dadson, S., Davidson, M.W., de Rosnay, P., Dorigo, W., Gruber, A., Hagemann, S., Hirschi, M., Kerr, Y.H., Lovergine, F., Mahecha, M.D., Marzahn, P., Mattia, F., Musial, J.P., Preuschmann, S., Reichle, R.H., Satalino, G., Silgram, M., van Bodegom, P.M., Verhoest, N.E., Wagner, W., Walker, J.P., Wegmüller, U., Loew, A., 2021. A roadmap for high-resolution satellite soil moisture applications – confronting product characteristics with user requirements. Remote Sens. Environ. 252, 112162. http://dx.doi.org/10.1016/j.rse.2020.112162, URL https://www.sciencedirect.com/science/article/pii/S0034425720305356.

Quintana-Seguí, P., Le Moigne, P., Durand, Y., Martin, E., Habets, F., Baillon, M., Canellas, C., Franchisteguy, L., Morel, S., 2008. Analysis of near-surface atmospheric variables: Validation of the SAFRAN analysis over France. J. Appl. Meteorol. Clim. 47 (1), 92–107. http://dx.doi.org/10.1175/2007JAMC1636.1, URL https://journals.ametsoc.org/view/journals/apme/47/1/2007jamc1636.1.xml.

Reichle, R., 2008. Data assimilation methods in the earth sciences. Adv. Water Resour. 31, 1411–1418. http://dx.doi.org/10.1016/j.advwatres.2008.01.001.

Reichle, R.H., De Lannoy, G.J.M., Liu, Q., Koster, R.D., Kimball, J.S., Crow, W.T., Ardizzone, J.V., Chakraborty, P., Collins, D.W., Conaty, A.L., Girotto, M., Jones, L.A., Kolassa, J., Lievens, H., Lucchesi, R.A., Smith, E.B., 2017. Global assessment of the SMAP level-4 surface and root-zone soil moisture product using assimilation diagnostics. J. Hydrometeorol. 18 (12), 3217–3237. http://dx.doi.org/10.1175/JHM-D-17-0130.1, URL https://journals.ametsoc.org/view/journals/hydr/18/12/jhm-d-17-0130_1.xml.

Reichle, R.H., Liu, Q., Koster, R.D., Crow, W.T., De Lannoy, G.J.M., Kimball, J.S., Ardizzone, J.V., Bosch, D., Colliander, A., Cosh, M., Kolassa, J., Mahanama, S.P., Prueger, J., Starks, P., Walker, J.P., 2019. Version 4 of the SMAP level-4 soil moisture algorithm and data product. J. Adv. Model. Earth Syst. 11 (10), 3106–3130. http://dx.doi.org/10.1029/2019MS001729, arXiv:https://agupubs.onlinelibrary.wiley.com/doi/pdf/10.1029/2019MS001729, URL https://agupubs.onlinelibrary.wiley.com/doi/abs/10.1029/2019MS001729.

Renard, B., Kavetski, D., Kuczera, G., Thyer, M., Franks, S.W., 2010. Understanding predictive uncertainty in hydrologic modeling: The challenge of identifying input and structural errors. Water Resour. Res. 46 (5), http://dx.doi.org/10.1029/2009WR008328, arXiv:https://agupubs.onlinelibrary.wiley.com/doi/pdf/10.1029/2009WR008328, URL https://agupubs.onlinelibrary.wiley.com/doi/abs/10.1029/2009WR008328.

Schneider, D.P., Deser, C., Fasullo, J., Trenberth, K.E., 2013. Climate data guide spurs discovery and understanding. Eos, Trans. Am. Geophys. Union 94 (13), 121–122. http://dx.doi.org/10.1002/2013EO130001, arXiv:https://agupubs.onlinelibrary.wiley.com/doi/pdf/10.1002/2013EO130001, URL https://agupubs.onlinelibrary.wiley.com/doi/abs/10.1002/2013EO130001.

Tramblay, Y., Bouvier, C., Martin, C., Didon-Lescot, J.-F., Todorovik, D., Domergue, J.-M., 2010. Assessment of initial soil moisture conditions for event-based rainfall–runoff modelling. J. Hydrol. (Amsterdam) 387 (3), 176–187.

Wakigari, S.A., Leconte, R., 2023. Exploring the utility of the downscaled SMAP soil moisture products in improving streamflow simulation. J. Hydrol.: Reg. Stud. 47, 101380. http://dx.doi.org/10.1016/j.ejrh.2023.101380, URL https://www.sciencedirect.com/science/article/pii/S2214581823000678.

Wanders, N., Bierkens, M.F.P., de Jong, S.M., de Roo, A., Karssenberg, D., 2014. The benefits of using remotely sensed soil moisture in parameter identification of large-scale hydrological models. Water Resour. Res. 50 (8), 6874–6891. http://dx.doi.org/10.1002/2013WR014639, arXiv:https://agupubs.onlinelibrary.wiley.com/doi/pdf/10.1002/2013WR014639, URL https://agupubs.onlinelibrary.wiley.com/doi/abs/10.1002/2013WR014639.

Wang, J., Zhou, L., Ma, C., Sun, W., 2023. How remote-sensing evapotranspiration data improve hydrological model calibration in a typical basin of qinghai-Tibetan Plateau Region. Hydrol. Earth Syst. Sci. Discuss. 2023, 1–26. http://dx.doi.org/10.5194/hess-2023-200, URL https://hess.copernicus.org/preprints/hess-2023-200/.

Yi, L., Yong, B., Chen, J., Zheng, Z., Li, L., 2021. Impact of 4D-var data assimilation on performance of the coupled land–atmosphere model WRF–TOPX: A case study of a flood event in the wangjiaba watershed, China. J. Hydrometeorol. 22 (3), 689–701. http://dx.doi.org/10.1175/JHM-D-20-0161.1, URL https://journals.ametsoc.org/view/journals/hydr/22/3/JHM-D-20-0161.1.xml.

Zhou, J., Wu, Z., Crow, W.T., Dong, J., He, H., 2020. Improving spatial patterns prior to land surface data assimilation via model calibration using SMAP surface soil moisture data. Water Resour. Res. 56 (10), n/a.

Zink, M., Mai, J., Cuntz, M., Samaniego, L., 2018. Conditioning a hydrologic model using patterns of remotely sensed land surface temperature. Water Resour. Res. 54 (4), 2976–2998. http://dx.doi.org/10.1002/2017WR021346, arXiv:https://agupubs.onlinelibrary.wiley.com/doi/pdf/10.1002/2017WR021346, URL https://agupubs.onlinelibrary.wiley.com/doi/abs/10.1002/2017WR021346.

Zribi, M., Dechambre, M., 2003. A new empirical model to retrieve soil moisture and roughness from C-band radar data. Remote Sens. Environ. 84 (1), 42–52. http://dx.doi.org/10.1016/S0034-4257(02)00069-X, URL https://www.sciencedirect.com/science/article/pii/S003442570200069X.